GEOCHEMISTRY, MINERALOGY AND PETROLOGY • SOFIA
ГЕОХИМИЯ, МИНЕРАЛОГИЯ И ПЕТРОЛОГИЯ • СОФИЯ
2008, **46**, 103-142.

Multiepisodic dyke systems in Hurd Peninsula, Livingston Island, South Shetland Islands Volcanic Arc (Antarctica): Petrological and geochemical implications for their magma evolution

Borislav K. Kamenov

Abstract. The numerous dykes occurring in Hurd Peninsula, Livingston Island are relics of the Mesozoic-Cenozoic magmatic arc of South Shetlands and their chronological, petrological and geochemical evolution is still not clarified unequivocally. The present contribution attempts to elucidate the dyke chronological sequences, mineral composition, nomenclature influenced by alterations, magma serial affinities, geochemical peculiarities, magma sources and magma evolution. Dykes are assigned to six magmatic pulses deduced out of their crosscutting relationships. The published K-Ar and $^{40}Ar/^{39}Ar$ ages in combination with our new field, petrological and geochemical results led to the distinction of three magmatic stages of dyke emplacement in Hurd Peninsula: (1) 80-55 Ma (I, II and partly III pulse); (2) 48-42 Ma (partly III and IV pulses) and (3) 40-31 Ma (V and VI pulses).

It is demonstrated that all TAS-classification nomenclatures of the dykes are deformed by alterations. The revised nomenclature applying immobile trace elements discards the transitional in alkalinity rock varieties and confirms the following suite of rocks: basalt – basaltic andesite – andesite – dacite – rhyodacite – rhyolite. The magma serial affinity of the dykes is predominantly tholeiitic, calc-alkaline high-alumina series being presented on a small scale. Unusually wide compositional range of plagioclases is registered, while clinopyroxene phenocrysts show restricted compositional range, corresponding to the different magmatic stages.

Substantial crystal fractionation is required to explain the geochemical characteristics of the dykes. The arc characteristics of the rocks are confirmed. The most distinctive features of the chondrite-normalized *REE* and MORB-normalized patterns are that they are depleted in compatible elements and moderately enriched in incompatible elements. The mantle source is characterized by the absence of residual garnet, depletion of HFSE prior to subduction and enrichment in *LILE* during arc genesis. Geochemical plots suggest that during magma-generation processes oceanic materials were involved (MORB-component) as well as a mantle source affected by subduction-related melts and fluids, sedimentary and crustal contamination (slab-derived components). Melting degrees are estimated geochemically as 5 to 40 % from fertile mantle source.

Some time-dependant geochemical ratios are revealed supporting a gradual increasing of basicity and alkalinity of the parental magmas along their age decreasing. A rough correlation between the degree of crustal contamination and the sequence of the dyke stages is evident also. The crustal component in the dykes decreases to the younger ages, according to the new geochemical data and the published isotope results, whereas notable contribution of subducted sediments and fluids to arc genesis in the same direction is established.

Key words: rock-forming minerals, geochemistry, petrology, dyke emplacement episodes, magma sources and settings

Address: Sofia University, 1000 Sofia, Bulgaria; E-mail: Kamenov@gea.uni-sofia.bg

Борислав К. Каменов. Многоетапни дайкови системи в полуостров Хърд, остров Ливингстън, вулканската дъга на Южношетландския архипелаг: Петроложки и геохимични следствия за геодинамичната еволюция

Резюме. Многобройните дайки, разкриващи се в полуостров Хърд на остров Ливингстън са реликти от мезозойско-неозойската магматична дъга на Южношетландските острови. Тяхната времева, петроложка и геохимична еволюция все още не е изяснена еднозначно. Настоящата публикация е опит за осветляване на хроноложката последователност, минералния състав, повлияната от променителните процеси номенклатура, магматичните сериални сходства, геохимичните особености, магматичните източници и магмената еволюция. Дайките са отнесени към шест магматични импулса, изведени от съотношенията им на пресичане. Публикувани K-Ar и ^{40}Ar/^{39}Ar възрасти, в съчетание с новите ни полеви, петроложки и геохимични резултати подкрепят разграничаването на три магматични етапа на дайково вместване в полуостров Хърд: (1) 80-55 Ma (I, II и частично III дайков импулс); (2) 48-42 Ma (III частично и IV импулс) и (3) 40-31 Ma (V и VI импулс).

Демонстрирано е, че всички TAS-номенклатури на скалите са деформирани от променителните процеси. Ревизираната номенклатура с приложението на неподвижни елементи-следи дискредитира скалните разновидности с преходноалкален характер и потвърждава следната скална последователност: базалт – андезитобазалт – андезит – дацит – риодацит – риолит. Магматичната сериалност на дайките е преобладаващо толеитова и в по-малка степен – калциево-алкална. Регистриран е необикновено широк размах в съставите на плагиоклазите, докато клинопироксеновите порфири показват ограничен състав, съответстващ на различните магматични етапи.

Геохимичните характеристики на дайките изискват съществено кристално фракциониране. Най-отчетливата особеност на хондрит-нормализираните *REE* и на MORB-нормализираните модели на разпределение е, че те са обеднени на съгласуващи се и са умерено обогатени на несъгласуващи се елементи. Мантийният източник се характеризира с отсъствие на гранат, изтощаване на HFSE до субдукцията и обогатяване на *LILE* по време на дъговото формиране. Геохимичните диаграми внушават, че по време на магмогенериращите процеси са били въвлечени океански материали (MORB-компонент), както и мантиен източник. Той е повлиян от свързани със субдукцията топилки и флуиди (произлезли от пластината компоненти) и замърсяване със седиментен и коров материал. Степените на частично топене от обогатен мантиен източник са оценени геохимично като 5 до 40 %.

Изявени са зависимости на някои геохимични отношения от хронологическата последователност на дайкообразуването, подкрепящи едно постепенно увеличаване на базичността и алкалността на родоначалните магми по посока на по-младите възрасти. Доказана е и корелация между степента на коровото замърсяване и времето на внедряването на дайките. Коровият компонент в дайките намалява към по-младите възрасти според новите геохимични данни и публикуваните вече изотопни резултати, като е установено и забележимо увеличаване на замърсяването на източника със субдуцирани седименти и флуиди в същото направление.

Introduction

Subduction of proto-Pacific ocean floor beneath the South Shetland Islands originated a Mesozoic-Cenozoic magmatic arc and most of the magmatic rock complexes in the islands are subduction-related. Numerous dykes cut all rock sequences and their concentration in Livingston Island, the second largest in the archipelago, is especially impressive. Neither their stratigraphic position is always known, nor are they fresh enough to apply their geochemical properties properly. In spite of the several attempts for unraveling the chronological relationships between the different dykes, their magmatic evolution is still not clarified in a reliable way. The sequence of the various in relative age and petrographic composition dyke episodes was identified up to now with ambiguity. One of the reasons leading to these problems is the lack of trustworthy petrological and geochemical data on the different dyke pulses. The present contribution aims to fill the gaps in our knowledge in this field with the hope that the magmatic dyke swarms in Hurd Peninsula could provide new arguments for geodynamic and magmatic interpretations. On the basis of the rich sample set, collected during the last ten years, an attempt is made to elucidate the field relations, mineral composition, nomenclature influenced by the alterations, magma serial affinities, geochemical peculiarities, magma sources and their evolution and to find new support for geodynamic reconstructions.

Geological background

Livingston Island contains the most complete record of the magmatic rock sequences, related to the activity of the Mesozoic-Cenozoic arc. Multiple hypabyssal plutonic and volcanic complexes are exposed there, amongst them many dykes. The island hosts several geological units, best exposed within Hurd Peninsula (Fig. 1).

The *Miers Bluff Formation* (MBF) building up the most of the Hurd Peninsula outcrops is a turbiditic metasedimentary sequence forming the local Basement of the arc (Hobbs 1968; Smellie et al. 1984, 1995). The depositional age of MBF has been debatable for a long time. It was assigned to Late Paleozoic (Grikurov et al. 1970), Triassic (Smellie et al. 1984; Willan et al. 1994; Onuyand et al. 2000), Early Jurassic (Herve et al. 1991), but recently it was accepted as Late Cretaceous (Stoykova et al. 2002; Pimpirev et al. 2006) on the basis of Campanian nannofossils. The *Mount Bowles Formation* is a volcanic sequence (Smellie et al. 1984) assumed to be of Cretaceous age on account of regional correlations (Smellie et al. 1995) or ^{40}Ar/^{39}Ar isochron dating (Zheng et al. 1996).

Plutonic rocks related to the magmatic arc compose several small stocks in the Hurd Peninsula (Hobbs 1968; Smellie at al. 1995; Kamenov 1997). Amongst them Hesperides Point Pluton (HPP) exposed along the west coast of the Peninsula was dated of 73±3 Ma (Kamenov 1997). The small plutonic outcrops along the eastern coast of Hurd Peninsula were interpreted as apophyses of the larger Barnard Point Batholith (BPB) of Eocene age (Kamenov et al. 2005). The tonalitic pluton BPB on the southeastern Livingston Island is composed of gabbro, diorite and possibly minor granodiorite (Caminos et al. 1973; Willan 1994; Smellie et al. 1996), but no detailed petrological and geochemical data are available for it.

Extension-related mafic volcanics known as Inott Point Formation (Pliocene-to Recent) are related to the opening of the Bransfield Strait back-arc basin (Smellie 2001; Veit 2002; Kamenov 2004). They consist of explosive and lava products of alkaline and tholeiitic affinity.

Different dyke swarms are present, cutting all previous rock formations with the exception of the Inott Point Formation volcanics (Kamenov 1999a, b).

Dyke intrusion episodes

About 350 dykes from Hurd Peninsula were recorded in the area of study and over 210 out of them were measured for their spatial orientation. 180 dykes were sampled and examined under microscope for petrographic description. 138 samples were analyzed for major oxides by wet silicate analysis, whereas 90 samples out of them were analyzed for trace elements by XRF method at Geochemical Laboratory of the “Geology and Geophysics” Co. in Sofia. Some small number of dyke samples (18) from the dated typical representative ones was reanalyzed at the Swiss Technological Institute (ETH) in Zurich by ICP-MS method on pellets.

Four well-developed maxima of the dyke swarm directions (Zheng et al. 2003) subdivided the dykes into four systems by their orientation (Fig. 1). Crosscutting mutual relationships between the dykes around the Bulgarian Antarctic Base in Hurd Peninsula were ground for their provisional separation initially into two groups: (a) “*the older*” and (b) “*the younger*”. We managed later on to identify six consequent dyke pulses, coming out of their crosscutting relationships. The relative age is

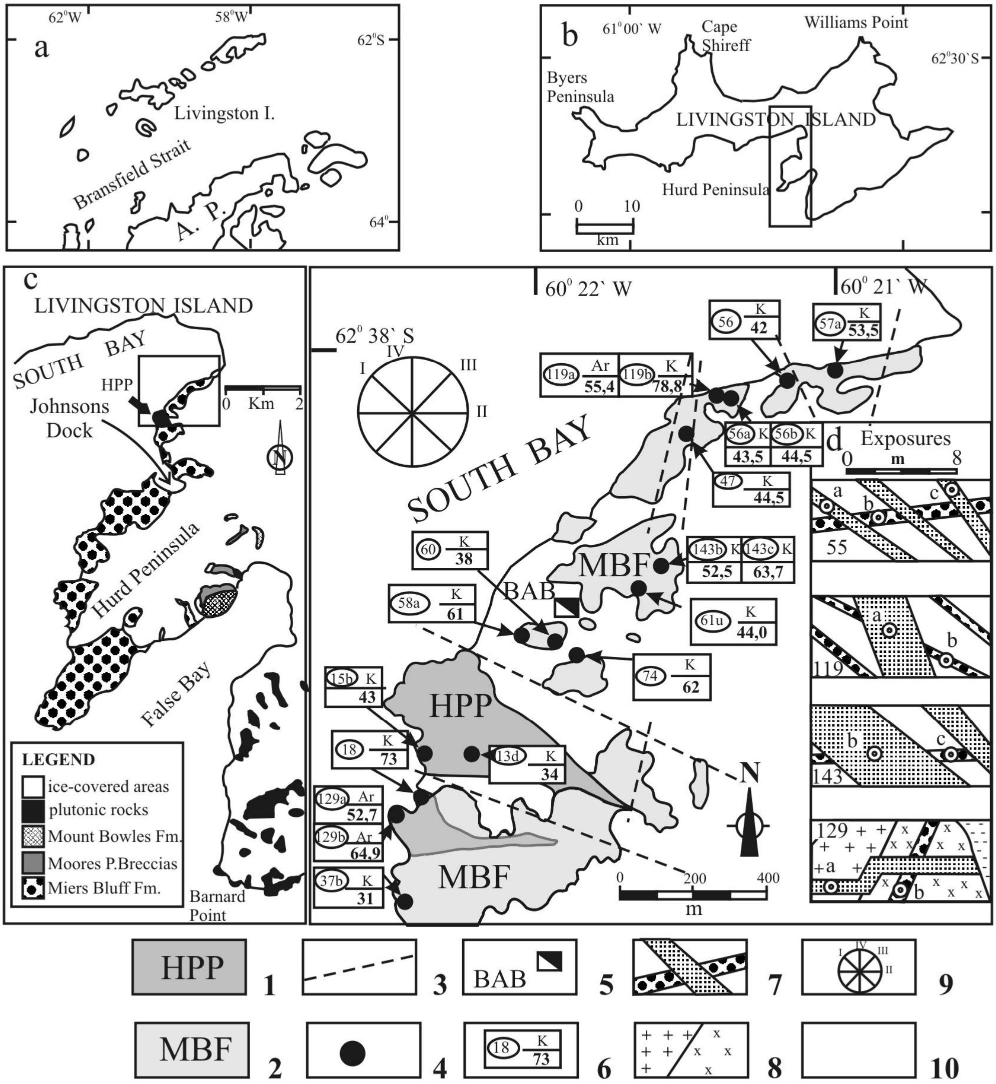

Fig.1. Sketch map of the distribution of dated dykes and some dyke exposures in Northwestern Hurd Peninsula (after Zheng et al. 2003): 1. Plutonic rocks of the Hesperides Point Pluton (HPP); 2. Miers Bluff Formation (MBF); 3. Faults; 4. Dated dykes; 5. Bulgarian Antarctic Base (BAB); 6. Sample number (above), age (below in Ma), and dating method (K: K-Ar; Ar: Ar-Ar); 7. Crosscutting relations in some of the dated dykes and sampling sites; 8. Quartz-diorite (+) and gabbrodiorite (x); 9. Main directions of the dykes; 10. Ice-covered areas. Insets a, b and c – location sketches

used as an important clue in assigning the dykes to these magmatic pulses. The spatial orientation of the dykes from the different intrusive pulses is often similar and vice versa, dykes from one and the same intrusive pulse may occupy more than one joint system. Obviously, the older tectonic trends have been reactivated during almost all later tectonic events. Comparing the available 27 isotope data for single dykes from the area (Grikurov et al. 1970; Willan & Kelley 1999; Zheng et al. 2003; Kraus et al. 2007) to the spatial trends of the dyke sets we did not establish any reliable and unequivocal correlation between the age and the spatial orientation. The correlation of the petrographic and major oxide composition of the dykes with their strike is also difficult and not always convincing. The same is valid for the trace element composition of the dykes, which is not diagnostic in all cases for a given dyke set by orientation. The separate dyke pulses include various petrographic nomenclatures, thus confirming the manifestation of magma differentiation inside of every dyke pulse. The dykes are referred to a particular dyke pulse with confidence only for examples in specific areas around the Bulgarian Antarctic Base, where the mutual crosscutting relationships provide unconditional proof for their relative age. In all other outcrops lacking clear relations between the dykes, the assignment to the established dyke pulses is provisional.

The dyke pulse I is presented for sure by only one dyke with a strike of 145° and thickness of 55 cm. The dyke is moderately altered andesite. It is cut by dykes of the second, third and fifth pulses. *The dyke pulse II* includes dykes emplaced predominantly in the tectonic trend 25° and having average thickness of 265 cm. The degree of alteration is significant. Strongly altered basalt, andesite and dacite with porphyry textures are the petrographic nomenclatures of the dykes from this pulse. Some of the dykes are displaced by tectonic fractures striking 150°. *The dyke pulse III* comprises several dykes intruded in the tectonic system around 150°, but single dykes of this pulse follow also the system 70-110°. The average thickness of the dykes is 320 cm. *The dyke pulse IV* is presented by numerous mainly mafic dykes striking around 150° which is nearly the same direction as in the first and third pulses dykes. Usually their thickness is smaller – average 90 cm. The rock varieties are basalt and basaltic andesite. The greatest part of the dykes is intensively altered and their detailed classification is problematic. *Dyke pulse V* is weakly developed in the area. The petrographic composition varies between basaltic andesite and andesite. The average thickness is over 400 cm. The main strike of the dykes from this pulse is close to 70°, like the one in some of the dykes from the third pulse. The alteration degree is low. *Dyke pulse VI* is presented by a single andesitic dyke with a strike of about 135°. The repetition of the tectonic systems 120-150° emplaced dykes (pulses I, III, IV and VI) is a proof that the geometry of the subduction zone, including its direction and its rate had been steady enough during the long periods of emplacement of the different dyke intrusions.

The already published geochronological isotope data on representative samples from all dyke pulses in combination with the here presented geochemical results may integrate the dyke pulses into three magmatic stages in a new way: (1) 80-55 Ma (the intrusive pulses I, II and partly III); (2) 48-42 Ma (the pulse IV and partly III); (3) 40-31 Ma (the intrusive pulses V and VI).They are considered as evolutional phases of the island arc development in Livingston Island. It seems that the dykes in the island began to be intruded close to the end of Late Cretaceous time and the dyke activity went to around Priabonian or even Oligocene time.

The emplacement episodes of the dyke activity in the eastern part of Livingston Island were discussed also by Willan & Kelley (1999). They gave proofs of the following magmatic phases: (1) ≈ 108-74 Ma; (2) 52-45 Ma; (3) 44-36 Ma; (4) 31-29 Ma. Zheng et al. (2003) based on some Ar/Ar and K/Ar dating of dykes especially from the ones exposed in Hurd Peninsula defined more accurately the span of the dyke activity covering the following stages: (1) 80-60; (2) 56-52; (3) 45-42; (4) 38-31 Ma. Kraus et al. (2005, 2007) did additional isotope dating on dykes from whole the archipelago and found a bit different periodicity in the dyke emplacement: (1) 65-60; (2) 57-53; (3) 48-43; (4) 40-37 Ma. The third and fourth episodes occurred everywhere in South Shetland Islands, but the first two stages are found only in Hurd Peninsula. This subdivision of the magmatic stages is not very different from the already published as far as the second and third magmatic stages are concerned, but the essential difference is in the first stage. It should be emphasized that in Hurd Peninsula some of the datings did not yield unequivocal results. Not always Ar-Ar data gave clear plateaus. This is especially true for the oldest K-Ar dates in Cretaceous time, which might be due to excess argon. There is a great probability they to be imprecise because of their advanced degree of alteration or determinations from not well separated mineral samples, challenging the reliability of these data. The suspicion that the earliest dating results are artificially old is one of the reasons the already yielded Campanian ages on some of the dykes to be considered problematic, the more so as a maximum age for the dykes is set by the Campanian nannofossils within MBF (Pimpirev et al. 2006). The similar geochemical properties of the dykes yielded ages between 80 and 55 Ma also supports the new view they to be included in one and the same intrusive stage.

Petrographic features

The mafic dykes prevail over the felsic ones in the area around the Bulgarian Antarctic Base. Usually they are subvertical and their thicknesses vary between 0.1 to 30 m, though they are normally thinner than 5 m. Analyzing only the number of the dykes in the different intrusive pulses we may note that the magma activity was weak at the dyke pulses I and II, increased and got to maximum during the emplacement of the dyke pulses III and IV and fade away during the last dyke events of V and VI intrusive pulses, when only single dykes occur. Generally speaking, the thickness of the dykes also grows in the same direction, confirming the opening of increasingly wider magma transferring channels with the maturity of the arc. The dominant emplacement mechanism is the one of the brittle deformations, reflected in the sharp and straightforward contact surfaces of the dykes, but even semi-plastic intrusions are met also rarely. The chilling margins of the dykes are normally about 1-2 cm, but sometimes several chilling zones form a common stripe 20-50 cm in width, containing several different in colour and density bands. The multiple emplacements of quickly following magma portions, as well as the kinetic flow differentiation might be the likely explanations for these peculiarities of the dykes. Amygdales are common in the central axial zone of the dykes and always filled with calcite, sericite, chlorite and quartz. The dykes range from almost aphyric (rare) to porphyritic (more commonly). The percentage of the phenocrysts in the bulk rock is normally around 20-30, but may become as large as 40-45 % in single cases.

Analyzed dykes comprise varieties from strongly undersaturated basic (normative olivine and nepheline exceeding 10 %, or presence of normative olivine and minor nepheline) through saturated or slightly oversaturated rocks and even to strongly oversaturated (10-25 % normative quartz) intermediate and acid nomenclatures (Table 1). The basic dykes have sometimes microphenocrysts, as well as glomeroporphyritic clusters of plagioclase and clinopyroxene. The composition of matrix is often difficult to distinguish due to the widespread alterations. In the rare cases of fresher samples, the groundmass is holocrystalline, composed predominantly of long lath-shaped labradorite to oligoclase, augite and iron-titanium oxides, distributed often in intergranular, intersertal or subophytic textures. The opaque minerals (magnetite, ilmenite, spinel, and titanite) are in subordinate amounts together with the accessory apatite and sometimes zircon. Variable amounts of secondary minerals occur. The basaltic andesites and andesites are more leucocratic and plagioclase in their assemblage is coarser-grained. Most of them contain small amount of quartz in the matrix. Pilotaxitic textures occur too. Sometimes hornblende is present in their mineral composition. Hawaiites and mugearite are mostly nonporphyritic or sparsely porphyritic dykes, slightly fissile in hand specimen due to

Table 1. *Selected chemical analyses of dated dykes from Hurd Peninsula*

Number	1	2	3	4	5	6	7	8	9
Rock	B*	A*	B*	Da	B	BA*	BA	BA*	A*
Age in Ma	78.8	64.9	63.7	62.0	61.0	55.4	53.5	52.7	52.5
SiO_2	46.61	58.96	45.84	62.66	47.79	54.60	50.79	50.68	57.85
TiO_2	1.19	1.16	1.43	0.49	0.70	1.33	1.30	1.83	0.75
Al_2O_3	15.62	15.52	17.50	14.73	17.61	15.21	15.70	15.49	16.41
Fe_2O_3	3.19	2.05	4.30	2.39	3.96	2.10	3.06	1.92	3.10
FeO	5.98	6.11	8.59	4.94	8.34	8.06	9.15	8.92	3.63
MnO	0.17	0.20	0.20	0.02	0.21	0.17	0.20	0.20	0.14
MgO	6.50	2.28	5.42	1.29	5.37	3.26	5.48	5.23	3.77
CaO	10.31	3.85	5.80	4.08	8.18	7.38	7.32	5.52	4.74
Na_2O	3.60	4.47	4.58	4.04	2.97	3.47	3.36	4.76	4.26
K_2O	1.97	2.04	1.49	2.10	1.27	1.23	0.96	1.51	2.70
P_2O_5	0.20	0.39	0.24	0.15	0.34	0.28	0.25	0.24	0.20
H_2O^-	0.17	0.17	0.12	0.09	0.06	0.07	0.08	0.07	0.20
LOI	4.72	2.64	4.01	2.54	2.74	3.20	2.32	3.25	2.41
Total	100.23	99.84	99.52	99.58	99.54	100.36	99.97	99.62	100.16
Cr	132	75	43	205	58	75	28	32	49
Ni	45	16	6	-	15	15	3	8	15
Co	32	7	39	-	26	23	30	32	17
Rb	50	24	42	110	45	28	25	38	47
Zn	540	113	96	-	390	95	102	106	70
Ba	610	280	500	270	170	260	260	400	680
Sr	1160	498	948	176	646	274	304	527	595
Zr	125	150	142	87	48	152	74	134	153
V	180	160	230	60	180	240	260	280	60
Nb	6	11	4	12	11	5	11	2	11
Y	25	46	26	47	21	28	18	24	30

the fluxional alignment of groundmass feldspars (the most abundant constituent). Microgranular textures are typical. Clinopyroxenes are finer-grained and magnetite is rather plentiful. Dacites are usually rare intensively altered leucocratic dykes. Most of them carry phenocrysts of coarse-grained albitized plagioclase and generally fewer pyroxene, hornblende and quartz. The groundmass shows sometimes microgranular felsitic texture.

Mineral composition

The mineral composition of the dykes is characteristic but not diagnostic for the different dyke pulses. 188 mineral microprobe determinations are the ground for these conclusions. The following rock-forming minerals are analyzed: olivine, plagioclase, clinopyroxene, amphibole, biotite, potassium feldspar and the secondary ones: talc, prehnite, epidote, calcite, chlorite, ilmenite, spinel, magnetite, and titanite.

Plagioclase phenocrysts in the dykes (Table 2) reveal that the compositional range is unusually wide – from oligoclase to anorthite. Most phenocrystals in the mafic dykes are normally zoned having calcic cores (An_{90}-An_{73}), progressing to An_{45}-An_{35} in the intermediate zones and An_{35}-An_{25} in the rims. Both oscillatory and reverse zoning in the anorthite composition of the intermediate zones occur rarer. These cases are especially more often observed in basaltic andesites from the "*older*" dyke group. Plagioclase microliths in the groundmass have compositions in the range An_{30}-An_{15}. The secondary alteration processes

Table 1. Continued

Number	10	11	12	13	14	15	16	17	18
Rock	A	B*	A	B*	BA*	A	Da	B*	B*
Age in Ma	44.5	44.5	44.0	43.5	43.0	42.0	38	34	31
SiO_2	57.53	47.50	59.55	45.25	49.76	52.57	68.99	46.32	45.24
TiO_2	1.34	1.03	1.18	0.97	1.10	0.58	0.55	0.47	1.18
Al_2O_3	14.65	15.46	14.66	17.10	17.17	16.18	14.45	17.78	17.35
Fe_2O_3	2.09	5.62	2.56	3.86	3.20	3.16	1.27	4.47	2.61
FeO	8.53	8.83	6.08	6.68	7.04	8.19	2.79	6.33	9.98
MnO	0.17	0.23	0.19	0.19	0.17	0.19	0.01	0.16	0.26
MgO	3.06	5.27	2.09	6.96	4.30	4.59	1.16	6.06	5.87
CaO	4.17	8.63	4.40	8.70	6.80	6.72	1.81	9.76	6.97
Na_2O	4.04	1.62	3.50	2.29	2.56	3.23	4.85	2.56	1.34
K_2O	2.28	0.36	2.04	2.77	4.34	1.20	2.52	1.01	2.65
P_2O_5	0.32	0.24	0.25	0.27	0.20	0.22	0.14	0.45	0.13
H_2O^-	0.18	0.16	0.19	0.12	0.17	0.04	0.14	0.08	0.31
LOI	1.23	4.69	3.35	4.70	3.17	2.77	0.94	4.14	5.67
Total	99.59	99.64	100.04	99.86	99.98	99.64	99.62	99.59	99.56
Cr	123	22	118	60	57	50	54	65	127
Ni	27	3	20	2	11	10	-	12	3
Co	33	18	2	2	16	17	-	28	17
Rb	69	21	69	47	90	35	111	29	83
Zn	102	101	96	142	97	98	-	467	275
Ba	480	20	350	340	790	280	550	270	260
Sr	360	297	305	320	917	452	171	947	240
Zr	241	45	129	148	41	92	230	50	107
V	110	320	30	250	110	170	20	250	110
Nb	13	11	11	11	12	9	7	12	12
Y	36	16	47	30	15	21	34	17	43

Notes: 1. Rock abbreviations (Le Maitre, 1989): B – basalt, BA – basaltic andesite, A – andesite, Da – dacite. The superscript * stands for strongly altered rocks. 2. Major oxides are analyzed in the Laboratory of the Department of Mineralogy, Petrology and Economic Geology at Sofia University "St. Kliment Ohridski" by wet silicate analyses. The trace elements are performed by RFA in the Laboratory of Geochemistry at "Geology and Geophysics" Co., Sofia

are responsible for all compositions under An_{15}. Transitional in alkalinity dykes contain bytownitic cores, when they are fresh (An_{82}-An_{75}) and pure albite (An_0-An_5), when altered. Labradorite-andesine plagioclase (An_{60}-An_{35}) is observed in basaltic andesites and andesites. Dacitic dykes contain more often albitized plagioclase phenocrystals.

Sometimes the large plagioclase phenocrysts contain aligned concentrically melt inclusions which may support magma mixing phenomena. The melt inclusions present in some of the plagioclases is indicative for their intratelluric history. Pressure release cracks in plagioclase phenocrysts indicate a very fast ascent of the melts. The concentration of phenocrysts around the axial zones of the dykes, as well of the amygdales there, evidences for a gravitational separation of early formed crystals in the magma chamber followed by injection of stratified magma into the dyke channel. The samples for geochemistry are selected from dykes with preserved primary composition of plagioclase.

Table 2. *Chemical compositions of selected plagioclases from dykes in Hurd Peninsula*

Rock	B		BA		B					BA
Notes	c	r	c	r	c	r	c	c	c	c
Sample	10	11	20	21	24	25	26	27	28	41
SiO_2	52.75	55.75	51.38	57.73	52.54	63.34	53.18	54.34	52.33	67.08
TiO_2	0.00	0.07	0.00	0.00	0.00	0.00	0.00	0.08	0.00	0.00
Al_2O_3	30.09	27.52	30.51	25.97	28.90	22.16	28.55	27.74	29.70	20.44
FeO	0.56	0.56	0.78	0.76	0.68	0.23	0.80	0.45	0.92	0.28
MnO	0.00	0.00	0.00	0.00	0.16	0.00	0,00	0,00	0.11	0.00
MgO	0.00	0.00	0.23	0.31	0.63	0.41	0.65	0.64	0.00	0.00
CaO	11.55	8.89	11.72	7.48	12.43	3.63	11.36	10.76	13.09	0.96
Na_2O	4.12	6.58	4.43	6.61	4.04	9.27	4.67	5.31	3.36	10.87
K_2O	0.61	0.66	0.67	0.64	0.46	0.86	0.32	0.42	0.43	0.00
Total	99.68	100.03	99.72	99.50	99.84	99.90	99.53	99.74	99.94	99.63
An %	58.30	41.00	57.00	36.70	61.00	16.70	56.60	51.50	66.70	5.10
Ab %	37.50	55.20	39.00	59.20	36.00	78.40	41.40	46.50	31.20	94.90
Or %	4.20	3.80	4.00	4.10	3.00	4.90	2.00	2.00	1.00	0.00

Notes: (c) core, (r) rim; Rock abbreviations: (B) basalt, (BA) basaltic andesite.

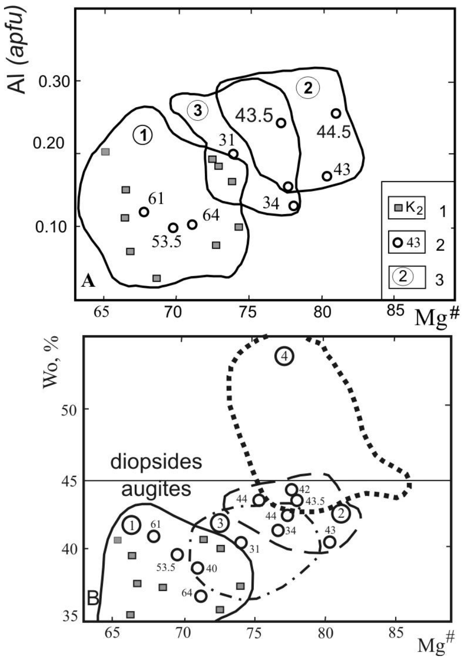

Fig. 2. A) Composition of clinopyroxenes in the system Al (*apfu*) *vs.* Mg$^{\#}$. The outlines of the fields only for the clinopyroxenes from the magmatic stages 1, 2 and 3 are shown. (1) Some individual analyses from the Upper Cretaceous volcanic formation Bowles and from the Late Cretaceous pluton HPP, (2) The individual empty circles are for the dated dykes with their age in Ma, (3) Magmatic stages; B) The clinopyroxenes in the plot wo % *vs.* Mg$^{\#}$. The field 4 is for clinopyroxenes from olivine basalts of Innot Point Formation plotted for comparison (Kamenov 2004)

Potassium feldspars are rich in orthoclase component monoclinic varieties met mainly in the later acid dykes, but observed also in small amounts in the intermediate dykes.

Clinopyroxene phenocrysts from all intrusive pulses, according to their relative and isotope age and from all chemically distinct varieties contain constantly some fresh relics, even in the most intensively altered samples (Table 3). The most striking feature of the clinopyroxene phenocrysts is the restricted range in their composition, corresponding to three divisions with typical fields of distribution (Fig. 2). It turned out that these fields are in conformity with the already defined magmatic stages of the dykes thus, the clinopyroxene composition is systematically changing with the age of the dykes. Therefore, the compositions of relic clinopyroxenes may provide not only a pointer to their original

Table 3. *Chemical composition of selected clinopyroxenes from dykes in Hurd Peninsula, Livingston Island*

Rock	B*	B*	A*	A*	BA	BA	BA*	BA*	BA	BA
Point	c-p	r-p	c-p	r-p	c-m	c-p	c-m	c-m	c-p	c-p
№	21	22	5	6	10	11	34	35	39	40
SiO_2	50.06	47.53	51.53	50.60	51.04	50.88	51.21	50.39	51.69	49.63
TiO_2	0.32	0.86	0.43	0.47	0.36	0.37	0.41	0.47	0.25	0.64
Al_2O_3	3.98	6.63	3.05	3.87	4.41	3.83	3.03	3.77	3.02	4.67
Cr_2O_3	0.26	0.09	0.19	0.00	0.12	0.12	0.00	0.00	0.56	0.00
FeO	6.35	9.58	8.38	9.26	9.28	11.63	8.87	8.74	6.76	10.19
MnO	0.00	0.12	0.28	0.25	0.20	0.24	0.12	0.24	0.12	0.23
MgO	16.71	14.17	15.60	15.02	15.56	14.82	15.36	15.57	16.41	15.15
CaO	20.79	20.53	20.13	20.42	19.13	18.11	20.67	20.64	20.67	19.33
Na_2O	1.03	0.98	0.00	0.00	0.00	0.00	0.00	0.00	0.40	0.00
K_2O	0.00	0.00	0.00	0.00	0.00	0.00	0.00	0.00	0.00	0.00
Total	99.50	99.10	99.59	99.89	100.10	100.00	99.67	99.82	99.88	99.84
Crystallo-chemical formulae										
Na	0.07	0.07	0.00	0.00	0.00	0.00	0.00	0.00	0.03	0.00
Ca	0.83	0.82	0.80	0.82	0.76	0.72	0.83	0.82	0.82	0.77
Mn	0.00	0.00	0.01	0.01	0.01	0.01	0.00	0.01	0.00	0.01
Fe^{2+}	0.10	0.11	0.19	0.17	0.23	0.27	0.17	0.17	0.15	0.22
Mg	0.00	0.00	0.00	0.00	0.00	0.00	0.00	0.00	0.00	0.00
M2	1.00	1.00	1.00	1.00	1.00	1.00	1.00	1.00	1.00	1.00
Fe^{2+}	0.10	0.18	0.07	0.12	0.06	0.09	0.11	0.10	0.06	0.10
Mg	0.93	0.79	0.86	0.83	0.86	0.83	0.85	0.87	0.90	0.84
Ti	0.01	0.02	0.01	0.01	0.01	0.01	0.01	0.01	0.01	0.02
Cr	0.01	0.00	0.01	0.00	0.00	0.00	0.00	0.00	0.02	0.00
Al	0.03	0.07	0.05	0.06	0.08	0.07	0.04	0.05	0.04	0.07
M1	1.08	1.06	1.00	1.02	1.01	1.00	1.01	1.03	1.03	1.03
Al	0.14	0.22	0.08	0.11	0.11	0.10	0.09	0.12	0.09	0.14
Si	1.86	1.78	1.92	1.89	1.89	1.90	1.91	1.88	1.91	1.86
T	2.00	2.00	2.00	2.00	2.00	2.00	2.00	2.00	2.00	2.00
$Mg^{\#}$	82.30	73.10	76.80	74.10	74.80	69.70	75.20	76.30	81.10	72.40
wo	42.30	43.20	41.70	42.30	39.80	37.70	42.30	41.80	42.50	39.90
en	47.40	41.60	44.80	42.80	45.00	43.40	43.40	44.40	46.60	43.50
fs	10.20	15.20	13.50	14.90	15.20	18.80	14.30	13.80	10.90	16.60
Stage	2	2	2	2	1	1	3	3	3	3

Notes: (c) core, (r) rim, (p) porphyry, (m) small crystal. Rock abbreviations as in Table 1. Stage – as in the text.

magma affinity, but also to the provisional age of the dykes up to the certain degree. The following divisions of clinopyroxenes are set apart (Table 4): *Division 1* incorporates the oldest dykes (80-55 Ma) comprising always augites with minimum Na and Cr *apfu*, relatively poorer in Al, with the lowest *wo* and *fs* components. The clinopyroxenes from the Late Cretaceous volcanics (Mount Bowles Formation) and plutonites (HPP) fall in the same field as well. *Division 2* clinopyroxenes are dispersed in Eocene age dykes (48-42 Ma) and they comprise augites with the highest $Mg^{\#}$ numbers, high *wo*-, low *fs*-components, high Cr and Al contents. *Division 3* clinopyroxenes occur as phenocrysts in the dykes of 40-31 Ma age. These dykes comprise mainly augites with intermediate values of $Mg^{\#}$ numbers and of

Table 4. *Chemical distinctions between clinopyroxene phenocrysts from the dykes of different magmatic stages in Hurd Peninsula, Livingston Island (average values)*

Stages	1	2	3
№ analyses	13	35	23
$Mg^{\#}$	72.6	78.1	74.4
wo	38.2	45.2	39.1
fs	17.2	11.6	15.2
Cr_2O_3	0.08	0.18	0.16
Al_2O_3	3.99	5.22	4.35
TiO_2	0.36	0.56	0.56
Na_2O	0	0.33	0.35
Rock nomenclature	*BA*	*B, A*	*B, BA*

Notes: $Mg^{\#}$ = 100 Mg/(Mg + Fe) in atoms per formula unit (*apfu*); (wo) and (fs) are wolastonite and ferrosilite components in per cent; Rock abbreviations as in Table 1

wo- and *fs* minals, but the highest Na and Ti contents are noted there. The composition of clinopyroxenes from Recent in age volcanics of the extensional tholeiitic and alkali basalts from Inott Point Formation (Kamenov, 2004) is shown on the Fig. 2B and referred provisionally as *division 4* clinopyroxenes for the sake of comparison only. The highest values of $Mg^{\#}$ numbers, *wo*-minal, Al., Ti and Cr are typical for composition of their diopsides. Tracing through the changes of the clinopyroxene composition with the age of the dykes, we could apprehend the modification of the magma sources and the partial magma evolution in this way. The gradual increasing of the amount of clinopyroxene from the earliest pulses dykes to the latest ones is a peculiar petrological feature of the dykes, correlated with a decrease of potassium-component in the feldspars and with the increasing of the $Mg^{\#}$ of the rocks.

The application of the discrimination method of Leterrier et al. (1982) to the clinopyroxenes analyzed (Fig. 3) reveals that the clinopyroxenes from division 1 fall mainly in the MORB field and partly in the orogenic basalt field (ORB), whereas the clinopyroxenes from the divisions 2 and 3 indicate mainly tholeiitic affinity of their magmas. The smaller part of the clinopyroxenes from division 1 fall in the orogenic field is predominantly of calc-alkaline and partly of tholeiitic character.

Amphiboles from the older intrusive dyke pulses are usually richer of Tschermak's component, while the amphiboles from the dykes of the later intrusive dyke pulses fall in the fields of richer in Si actinolite and hastingsite with relative increased amount of alkalis in their composition.

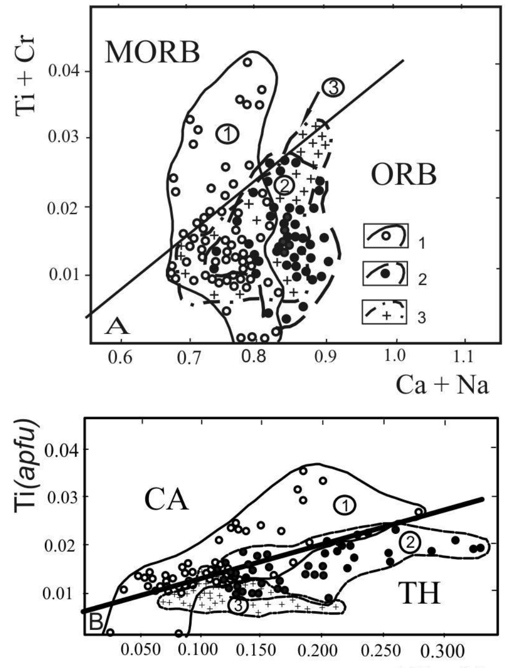

Fig. 3. Discriminant diagrams for analyzed clinopyroxenes (Leterrier et al. 1982): A) Ti+Cr *vs.* Ca+Na (*apfu*) plot. (1), (2) and (3) fields for dyke stages, (MORB) pyroxenes from middle ocean ridge basalts, (ORB) pyroxenes from orogenic basalts; B) Ti *vs.* Al (*apfu*) plot. Series: (CA) calc-alkaline, (TH) tholeiitic

Magnetites are dominantly high-Ti, high-V, low-Cr, moderately-Al and Ca-bearing varieties. *Ilmenite* shows moderate contents of Mn and usually is very scarce.

Alteration

The dykes studied are variably altered, usually moderately to strongly. Both phenocrysts and groundmass are sometimes intensively transformed to secondary products. There are dykes almost completely transformed and built up exclusively by secondary minerals. Plagioclases are sometimes deanorthitized and their relatively high contents of Na_2O and K_2O may be due partly to the large scale by the presence of sericite and albite. The clinopyroxenes are more stable to the alterations and most often they are replaced irregularly partially by chlorite and calcite, but leaving some unaltered relics. The opaque minerals often are deformed into aggregate of titanite, rutile and iron-bearing hydroxides. The most often secondary minerals are calcite, chlorite (picnochlorite, prochlorite and clinochlor), sericite and relatively rarer observed ones are epidote, albite, quartz, talc, zeolites, scapolite, adularia, prehnite and clay minerals. The secondary minerals (Table 5, Table 6) are indicative for hydrothermal propylitic type alteration. Calcite, epidote or quartz veinlets sometimes cut the

Table 5. *Chemical composition of selected secondary minerals from dykes in Hurd Peninsula, Livingston*

Rock	B	B	Ap	Ap	BA*	BA*	BA*	B	vein
Mineral	Tc	Pr	Pr	Pr	Pr	Pr	Pr	Ep	Cal
№	1	2	3	4	5	6	7	8	10
SiO_2	60.89	42.56	42.03	42.45	44.75	42.66	46.20	38.49	2.58
TiO_2	0.00	0.00	0.06	0.06	0.00	0.00	0.00	0.00	0.10
Al_2O_3	0.82	19.74	23.94	24.15	23.43	21.34	21.25	23.87	1.35
FeO	4.36	5.07	0.70	0.71	3.43	5.91	2.93	12.32	1.10
MnO	0.00	0.00	0.00	0.00	0.08	0.19	0.21	0.30	0.59
MgO	29.38	0.00	0.00	0.00	0.00	0.00	0.00	0.00	1.51
CaO	0.17	26.49	26.22	26.49	24.30	24.62	24.45	23.45	51.04
Na_2O	0.00	0.00	0.00	0.00	0.35	0.00	0.00	0.00	0.08
K_2O	0.00	0.00	0.00	0.00	0.00	0.63	0.00	0.00	0.10
L.O.I.	4.37	6.14	7.05	6.14	3.66	4.65	4.96	1.57	41.55
Total	95.63	93.86	92.95	93.86	96.34	95.35	95.04	98.43	58.45
Crystallo-chemical formulae									
Si	3.92	3.07	2.98	2.98	3.07	3.03	3.20	3.23	
Al	0.06	0.93	1.02	1.02	0.93	0.97	0.80	2.36	
Σ T	3.98	4.00	4.00	4.00	4.00	4.00	4.00	-	
Al	0.00	0.74	0.98	0.98	0.97	0.82	0.93	-	
Mg	2.82	0.00	0.00	0.00	0.00	0.00	0.00	0.00	0.008
Fe	0.24	0.31	0.04	0.04	0.20	0.35	0.17	0.86	0.105
Ca	0.01	2.04	1.99	1.99	1.79	1.87	1.81	2.11	0.910
Mn	0.00	0.00	0.00	0.00	0.00	0.01	0.01	0.02	0.008
Ti	0.00	0.00	0.00	0.00	0.00	0.00	0.00	0.00	
Na	0.00	0.00	0.00	0.00	0.05	0.00	0.00	0.00	
K	0.00	0.00	0.00	0.00	0.00	0.06	0.00	0.00	
Total	3.07	3.09	3.01	3.01	3.01	3.11	2.92	-	
Σ cations	7.05	7.09	7.01	7.01	7.01	7.11	6.92	8.59	

Notes: 1. Rock abbreviations as in Table 1, (Ap) aplite, (vein) hydrothermal vein. 2. Mineral abbreviations: (Tc) talc, (Pr) prehnite, (Ep) epidote, (Cal) calcite. 3. The calcite is composed of 0.75% Mg, 0.90% Fe, 0.75% Mn and 85.85% $CaCO_3$.

dykes or fill the cavities. Chlorite and epidote are developed predominantly on the central cores of the plagioclases. The alterations are low-temperature and realized at high P_{H2O}. Some of the secondary products are thought to have formed to deuteric rather than metamorphic process (Smellie et al. 1984). Willan (1994) supports the idea that the hydrothermal vein swarm in Hurd Peninsula is of hydraulic origin and it is probably coeval with the Late Cretaceous volcanism

The abundant magmatic events in this small area obviously affected thermally the dykes that are low-grade metamorphosed in pumpellyite-prehnite facies.

It seems that the samples discussed in the paper are the most preserved among the dykes of the studied area, but it is safe to state that it is almost impossible completely fresh specimens to be found. This is of importance especially for the earliest dyke pulses, which are more intensively altered than the latest ones. All stated alteration characteristics of the dykes should be taken into consideration when their chemical composition is the basis of classification procedures, but unfortunately this was not the case up to now. Geochemical interpretations are also dependable on the appropriate estimation of the problem whether the studied samples have undergone mass exchange or not.

Table 6. *Chemical composition and atomic components per formula unit of selected chlorites from dykes in Hurd Peninsula, Livingston (oxygen base)*

Rock	BA*	BA*	BA*	Da	Da	BA	BA*	BA	BA	B*
№	4	5	7	8	9	10	11	12	14	15
SiO_2	27.26	27.51	27.43	25.40	27.00	27.90	28.32	28.13	24.41	28.15
TiO_2	0.00	0.00	0.00	0.00	0.00	0.00	0.00	0.00	0.22	0.00
Al_2O_3	16.97	17.81	16.82	19.22	18.10	17.36	18.37	16.41	14.18	18.46
FeO	30.73	27.13	29.32	33.41	31.90	21.81	29.12	28.86	37.56	22.29
MnO	0.39	0.35	0.30	1.09	0.44	0.39	0.38	0.49	0.42	0.45
MgO	12.58	15.16	14.98	9.16	11.09	19.52	13.68	14.07	10.61	18.32
CaO	0.20	0.09	0.05	0.09	0.21	0.09	0.23	0.00	0.13	0.21
Na_2O	0.65	0.00	0.00	0.00	0.00	0.76	0.00	0.00	0.00	0.00
K_2O	0.00	0.00	0.12	0.00	0.00	0.00	0.00	0.00	0.00	0.00
Total	88.78	88.05	88.85	88.37	89.74	87.83	90.10	87.96	87.53	87.88
L.O.I.	11.22	11.95	11.15	11.63	10.24	12.17	9.90	12.04	12.47	12.12
$Mg^{\#}$	42.4	50.0	47.9	33.1	37.5	61.7	45.8	46.8	33.7	59.7
Numbers of cations on the basis of 18 oxygens										
Si	2.93	2.91	2.91	2.79	2.89	2.89	2.95	3.01	2.80	2.91
Al	1.07	1.09	1.09	1.21	1.11	1.11	1.05	0.99	1.20	1.09
Z	4.00	4.00	4.00	4.00	4.00	4.00	4.00	4.00	4.00	4.00
Al	1.08	1.13	1.02	1.28	1.18	1.01	1.20	1.08	0.72	1.16
Mg	2.02	2.39	2.37	1.50	1.77	3.02	2.12	2.25	1.82	2.82
Fe	2.76	2.40	2.60	3.07	2.95	1.89	2.54	2.58	3.61	1.93
Mn	0.04	0.03	0.03	0.10	0.04	0.03	0.03	0.04	0.04	0.04
Ca	0.02	0.01	0.01	0.01	0.02	0.01	0.03	0.00	0.02	0.02
Ti	0.00	0.00	0.00	0.00	0.00	0.00	0.00	0.00	0.02	0.00
Y	5.92	5.96	6.03	5.96	5.96	5.96	5.92	5.95	6.23	5.97
“fm”	0.58	0.50	0.55	0.67	0.63	0.38	0.54	0.53	0.66	0.40

Notes: 1. Rock abbreviations as in Table 1. 2. $Mg^{\#}$ = 100 Mg/(Mg + Fe); “*fm*” = Fe/(Fe + Mg). 3. The loss of ignitions (L.O.I.) is estimated as a difference between a hundred per cent and the totals of the microprobe analysis. 4. Analyst: C. Stanchev, “Geology and Geophysics” Co., Sofia.

To screen elements that may have been mobile during secondary processes we apply several tests. Plotting each element against some index of alteration intensity was the first step in this procedure. The loss of ignition (LOI) value was used as a useful indicator for the degree of alteration because the transformation of minerals and the hydration of glass raise the volatile contents. The average values of LOI (normally over 4 wt. %) are the highest in the earliest dyke pulses and gradually decrease to the latest ones. No significant correlation between the LOI and the trace elements Y, Ti, Nb and Zr is established and the position of samples on these diagrammes (not shown here) is independent on alteration intensity, which is a proof for their immobile character during the hydrothermal alterations.

The examination of the correlation matrix for all elements that should behave incompatibly during the alterations shows that for a pair of some of these elements the correlation coefficient is high – that is the ratio of these elements is unlikely to have been changed by alteration. However, inexplicable loss of correlation may indicate that at least one of the participating elements was mobile. K_2O and Zr (Fig. 4A) show a positive correlation in fresh samples, but not in the altered ones. The lack of correlation for the whole set of samples supports the inference that K was mobile and its use in the classical TAS-diagramme is inappropriate for this case. The redistribution of the primary amounts of the alkalis would deform the classical classification procedures. Consequently, for geochemical and classification purposes the help of some immobile trace-elements should be sought. Quite opposite is the case of putting together Nb *vs.* Zr (Fig. 4B) or Nb *vs.* Y and Zr *vs.* Y (not shown) – a strong positive correlation between these elements in fresh and altered dykes is established. Therefore, these elements were unaffected by weathering and metamorphism and probably have been with immobile behaviour.

The impact of the hydrous fluids on the dykes might be estimated also by using the method of Davies et al. (1978) on the ternary diagramme MgO-SiO_2-CaO/Al_2O_3 (after Schweitzer & Kröner 1985) shown in Fig. 5. Almost all samples plot well inside the field of the relatively low degree of alteration with respect to these major oxides. It means that the alterations in these samples do not influence

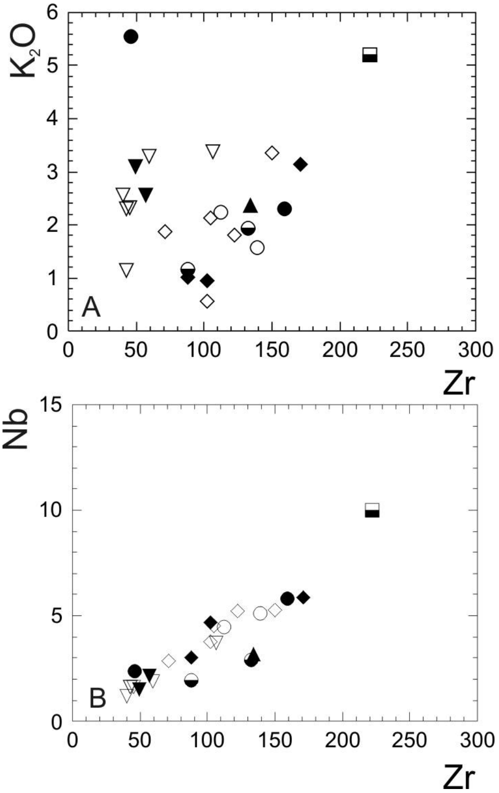

Fig. 4. A) K_2O *vs.* Zr plot of dykes showing the lack of correlation and the mobile behaviour of potassium due to alterations; B) Nb *vs.* Zr plot. The strong positive correlation evidences the immobile behaviour of the both trace elements. The solid symbols are for dated dykes. The specific symbols for the dyke pulses are as follows: (I) semi-filled square, (II) circle, (III) rhomb, (IV) triangle turned down, (V) semi-filled circle, (VI) triangle turned up

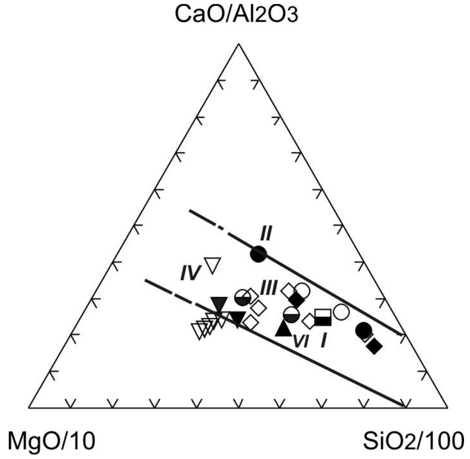

Fig. 5. The ternary diagram MgO/10-CaO/Al_2O_3-SiO_2/100 (Davies et al. 1978, cited after Schweitzer & Kröner 1985) for dykes of different dyke pulses is used to separate the intensively altered dykes with significant input (outside of the belt from the apex SiO_2/100 towards the face MgO-CaO/Al_2O_3 of the triangle). The symbols correspond to those in Fig. 4

essentially to their geochemical properties. The small number of exceptions plotting outside this field is all from the dyke pulse IV. They features very high LOI (4.40-7.10 %) reflecting their strong alteration, which may have also affected the immobile trace elements.

The results of the applied tests show that the reliable for geochemical studies trace-elements with immobile behaviour for this case are Nb, Y, Zr, and Ti.

Nomenclature problems

Major oxides show considerable scatter of their compositions (Table 1). Dykes that are relatively fresh (LOI< 2 wt. %) and the ones that are altered to a large degree (LOI>4 wt. %) sometimes have comparable distributions, thus appearing that they probably can be used to estimate the primary effects. However the classification is risky when the samples are very heavily influenced by the fluids as the case in some of the applications of the standard TAS-diagrammes is. A classification attempt using the TAS-diagramme is shown in Fig. 6. The field of all analyzed dykes was constructed on the base of 138 samples from Hurd Peninsula. It is clear that the dated specimens cover the whole compositional diversity of the set and includes all intrusive pulses.

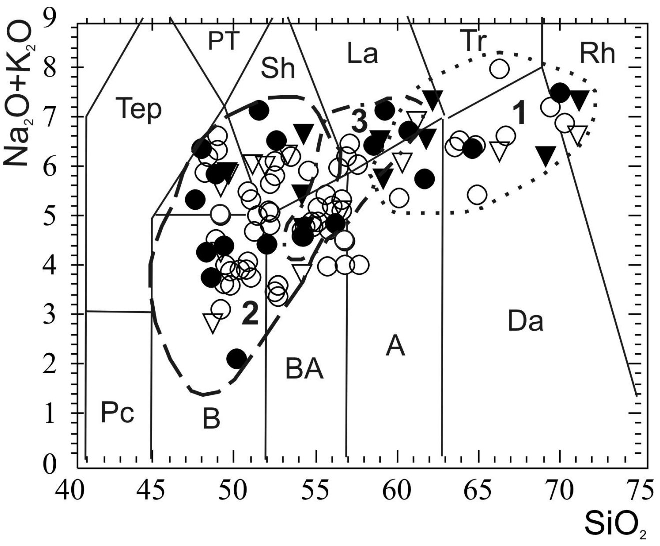

Fig. 6. Total alkalis vs. SiO_2 (TAS) clas-sification diagram (Le Maitre et al. 1989) for sampled dykes from Hurd Peninsula. Symbols: solid cycles – dated dykes (Zheng et al. 2003); solid triangles – dated dykes (Kraus et al. 2007); open cycles – samples with geochemistry only, this contribution; open triangle – samples with geochemistry only (Kraus et al. 2007). Outlined fields: (1) magma-tic stage 1, (2) stage 2, (3) stage 3. Abbreviations of the nomenclature: (Pc) picrobasalt, (Tep) tephrite, (PT) phono-tephrite, (B) basalt, (Sh) shoshonite, (BA) basaltic andesite, (A) andesite, (La) latite, (Da) dacite, (Tr) trachite, (Rh) rhyolite. Take a note of the several samples falling outside the fields 2 and 3 because of an unreliable assigning to the certain age relations

Three fields can be delineated enveloping the main magmatic stages, defined by geochronological dating. The first field includes predominantly samples of pulses I and II and partially from pulse III, falling mainly in the nomenclatures of andesite, dacite and rhyolite. Single points are latite species. The second field covers dominantly samples from pulse IV and partially from pulse III – basalts, K-trahybasalts, basaltic andesites, shoshonites and rarely hawaiites and mugearites. All these are more or less basic rocks, but this field is strongly elongated along the values of the alkalis. The scatter seems to be unnatural for some process of crystallization differentiation because is done to the direction of the most mobile major oxides like the alkalis. More over, just the dykes from the pulse IV have the highest degree of alteration and contain the highest LOI values. The relatively high degree of alteration in the dykes cast suspicion on the correct primary position of the transitional in alkalinity samples like potassium trahybasalts, shoshonites, hawaiites and latites. The third field unifies a few samples from the pulses V and VI, assigned to the basaltic andesites, andesites and latites. Only samples assigned to an individual dyke pulse with certainty are included into the fields of the magmatic stages. Taken as a whole, the attempt supports a range in the frames of the basic, intermediate and acid group magmatic rocks, but introduces uncertainty at the delimitations of the transitional in alkalinity rocks.

The weak points of the traditional TAS-classification could be eliminated if we use the immobile trace-elements for classification purposes. Our result of the application of the method of Winchester & Floyd (1977) is shown in Fig. 7, where the ratio Zr/TiO_2 is used as a reliable differentiation index. A clear correlation is manifested between the SiO_2 and the ratio Zr/TiO_2. The variations in the composition of the dykes are very homogeneous and more compact than in the TAS-plot and no transitional in alkalinity varieties are present.

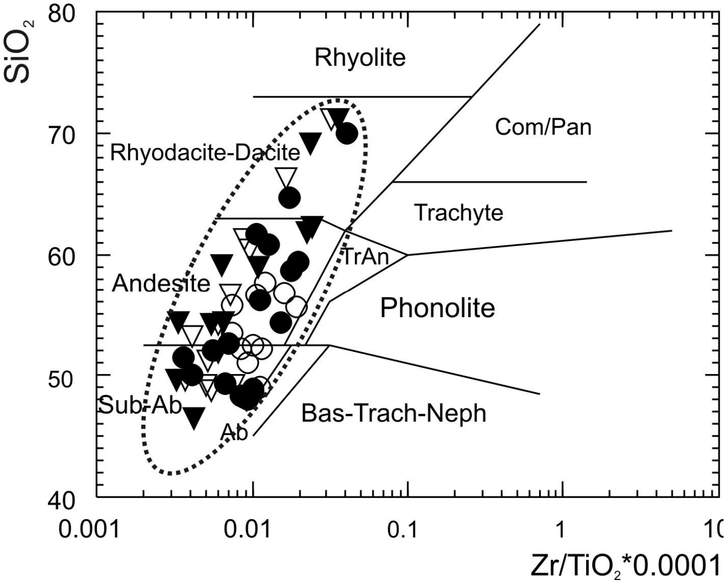

Fig. 7. Dykes from Hurd Peninsula in the plot SiO_2 *vs.* Zr/TiO_2 (Winchester & Floyd 1977). Rock abbreviations: (Sub-Ab) subalkali basalts, (TrAn) trachyandesite, (Bas) basanite, (Trach) trachite, (Neph) nephelinite, (Com/Pan) comendite-pantellerite. The sample symbols are as in Fig. 6

The original diagramme of Winchester, Floyd (1977) SiO_2 *vs*. Nb/Y has been modified by Kraus et al. (2007) replacing the SiO_2-boundaries delimiting the fields within calc-alkaline series with nowadays widely accepted horizontal straight-running boundaries as used in the TAS-diagramme (LeMaitre 2002). Our samples plotted on this diagramme (Fig. 8) fall entirely in the normal subalkaline series and this result we think is more reliable than the obtained on the classical diagrammes based on major elements only. Therefore, the assumption that some samples owe their high content of alkalis by secondary postmagmatic processes is plausible. The rocks like latite, potassium trachybasalt, shoshonite, mugearite and hawaiite are not confirmed too. The final conclusion of these attempts is that the dykes from Hurd Peninsula could be referred only to the fields of the normal suite and that the transitional varieties are possibly artificial nomenclatures due to the alterations.

Magmatic series

The classification diagrammes with SiO_2 as well as with Zr/TiO_2 ratio as indexes of differentiation define subalkaline series for dykes in Hurd Peninsula. The classical way of the distinction between the calc-alkaline and tholeiitic affinity of these subalkaline series is to use the diagramme of Peccerillo & Taylor (1976) and it is applied here with the extension of the Dabovski et al. (1991). Two branches are seen for the dyke samples in Fig. 9. One of them is located within the transitional area between the calc-alkaline and high-potassium

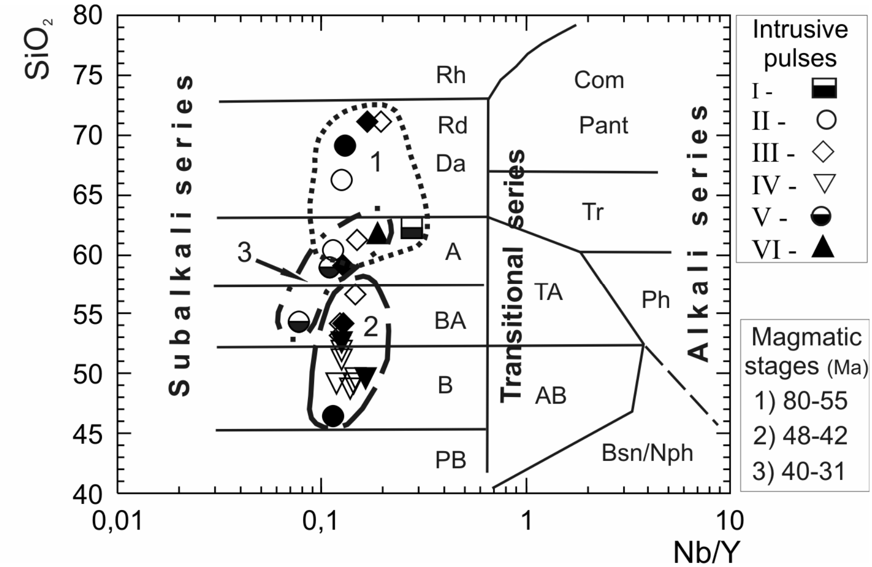

Fig. 8. Classification diagram SiO_2 *vs*. Nb/Y (Winchester & Floyd 1977) modified by Kraus (2005) to harmonize the nomenclature with the present-day limits of the classification fields (LeMaitre 2002). Only selected samples with reliably determined affiliation to the specific dyke pulses are plotted. The chronological ranges of the magmatic dyke stages are put down right. Abbreviations for the rock nomenclature: (PB) picritic basalt, (B) basalt, (BA) basaltic andesite, (A) andesite, (Da) dacite, (Rd) rhyodacite, (Comm) comendite, (Pant) pantellerite, (Tr) trachite, (Ph) phonolite, (TA) trachyandesite, (AB) alkali basalt, (Bsn/Nph) basanite-nephelinite

calc-alkaline series. The second branch is almost vertical and reflects steep and large change of the K_2O contents, crossing the series CA, HKCA, SH and UKSH. With the exception of the “tephrite” from the pulse II and the “latite” from the intrusive pulse I, all other points of this branch are assigned to pulse IV. Obviously, the unusual orientation of this branch is not a primary peculiarity, but similarly a consequence of the mobility of K_2O in postmagmatic conditions. The same reason is obstructive of using the ternary AFM-plot of Irvine & Baragar (1971) for the discrimination of the magma affinity.

The uncertainty in the determination of the magma seriality originates, as in the other classification schemes, again from the alterations of the dykes. Under these circumstances a diagramme based on the immobile elements Zr and Y, after MacLean & Barrett (1993) is applied (Fig. 10). The predominant part of the dykes fall on the tholeiitic field. Only small number samples are included into the transitional series (some samples from the pulses I and III, as well as some altered strongly basalts and basaltic andesites). Similar is the distribution of the samples in the diagramme of Miyashiro (1974) of the sort FeO_T/MgO *vs.* SiO_2, demonstrated in Fig. 11. All analyzed dykes are again within the field of the tholeiitic affinity, taking into consideration that the delimitations in the plot are valid, only for the intermediate degrees of differentiation (i.e. $2.0<FeO_T/MgO<5$, according to the initial requirement of Miyashiro (1974). The more homogeneous and compact distribution of the samples on the both plots (namely Y *vs.* Zr and FeO_T/MgO *vs.* SiO_2) than on the diagramme K_2O *vs.* SiO_2 demonstrates that the elements

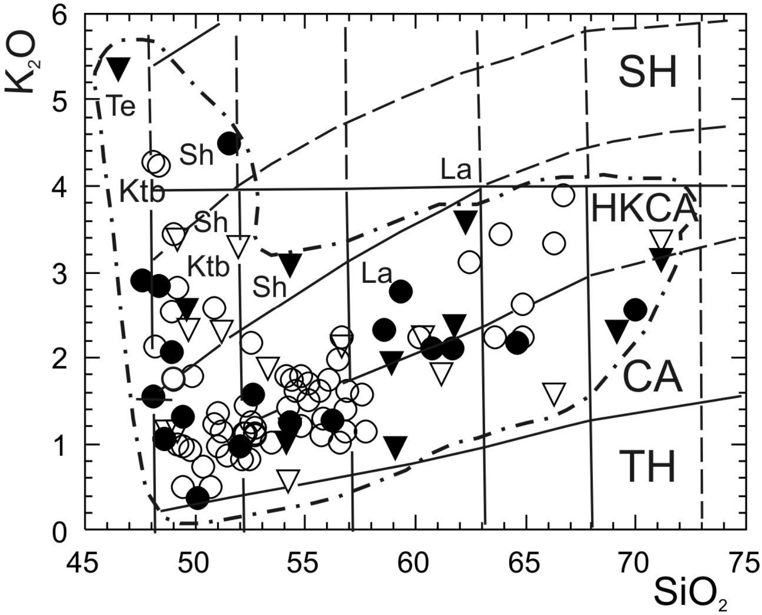

Fig. 9. Serial trends in SiO_2 *vs.* K_2O diagram (Peccerillo & Taylor 1976) expanded (dashed lines) by Dabovski et al. (1989). Series: (TH) tholeiitic, (CA) calc-alkaline, (HKCA) high-potassium calc-alkaline, (SH) shoshonitic. The meaning of the sample symbols is the same as in Fig. 6. Some of the intensively altered samples on the upper part of the diagram are named with the following abbreviations: (Te) tephrite, (Ktb) K-trachybasalt, (Sh) shoshonite, (La) latite. The nomenclature is after LeMaitre (2002)

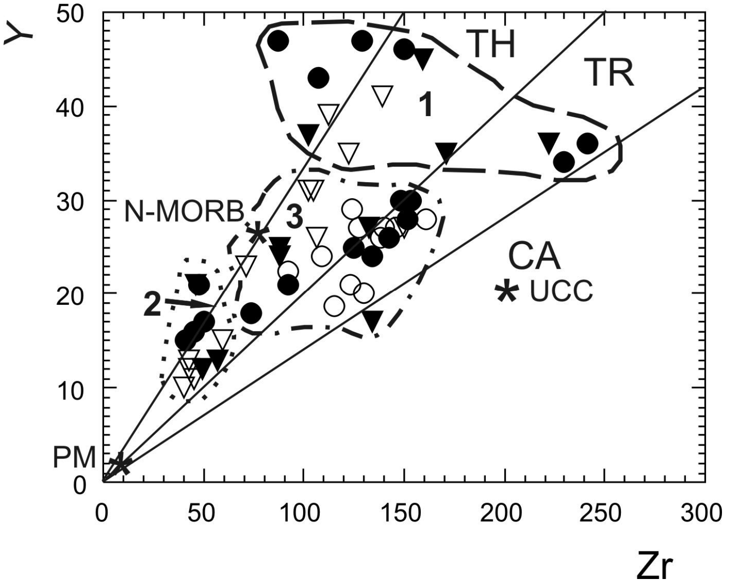

Fig. 10. Serial affinity of dykes from Hurd Peninsula in the plot Zr *vs.* Y (MacLean & Barrett, 1993). The average values of the primitive mantle (PM) are after McDonough & Sun (1995), of N-MORB – after Sun & McDonough (1989) and of the upper continental crust (UCC) are after Rudnick & Gao (2003). Series: (TH) tholeiitic, (TR) transitional alkaline, (CA) calc-alkaline. The sample symbols are as in Fig. 6

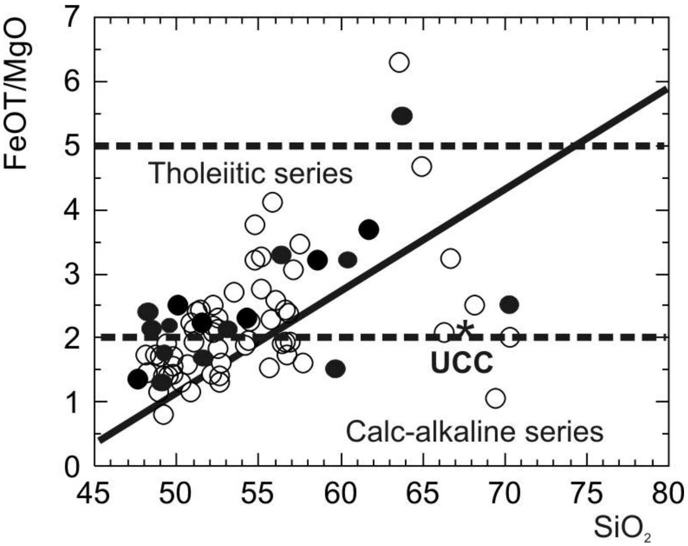

Fig. 11. Serial affinity of dyke samples from Hurd Peninsula in the plot SiO_2 *vs.* FeO_T/MgO (Miyashiro 1974). UCC – upper continental crust (Rudnick & Gao 2003). The solid symbols are for the dated rocks and the open – for dykes with uncertain age affiliation

with strong immobile behaviour reflect more reliably the initial magma composition in comparison to the serial diagramme based on the more mobile elements.

Usually the basalt members of the calc-alkaline series are high-Al basalts (Wilson 1989) and then their Al_2O_3 contents are in the range 16-20 wt. %. The analyzed basalts and basaltic andesites from the Hurd Peninsula for their most part satisfy the criteria for the high-Al calc-alkaline basalts and only a little part out of them are referred to the tholeiitic series (Fig. 12). This result is contradictory to the immobile trace-element systematic pointing to the tholeiitic affinity for the predominant part of the dykes. Possible explanation for this lack of correspondence is the accumulation of plagioclase phenocrystals. Most of the samples in the field of the high-Al basalts belong to the pulse IV, which is strongly porphyritic. The amount of the porphyry generation, consisting mainly of plagioclase, is rather high (up to 40-50 %) and it is reflected to the assignment to the calc-alkaline, but not to the tholeiitic affinity of these samples. Thus, this affinity for the samples with high alumina contents is a result of accumulation and it is not a primary magma peculiarity.

Most of the K/Rb ratios in the dykes fall within the ratios characteristic of calc-alkaline rocks at continental margins. The influence of the mobile behaviour of K on these results can not be denied. Only the most primitive and moderately evolved dykes show significantly higher K/Rb ratios than is normal for continental rocks (their average values for Eocene in age dykes is 385, close to the ratios typical for the tholeiitic rocks). The tholeiitic trend of the dykes might be a trace of the subducted relatively young and hot oceanic crust (N-MORB) beneath the continental margin of the Antarctic plate.

Geochemistry

REE patterns

The elements from the lanthanide group are the least soluble trace elements and usually they are relatively immobile during the low-grade metamorphism and hydrothermal alterations. Having in mind that their patterns of chondrite-normalized distribution are controlled by *REE* composition of the magma source, the degree of partial melting and crystal fractionation, we constructed diagrammes separately for the selected representative samples from the different intrusive dyke pulses.

The *LREE*-fractionation over *HREE* is moderate for the samples from the pulses I and II (Fig. 13A). Fractionation factor between *LREE* and *HREE* $(La/Lu)_N$ is 5x for the “latite” from the pulse I. The enrichment of La in comparison to the chondrite is about 90, while the one for Lu does not exceed 18.x. This factor is smaller in the representative samples of the pulse II – 3.3 to 3.5. In all these patterns, excluding the one of the strongly altered basalt

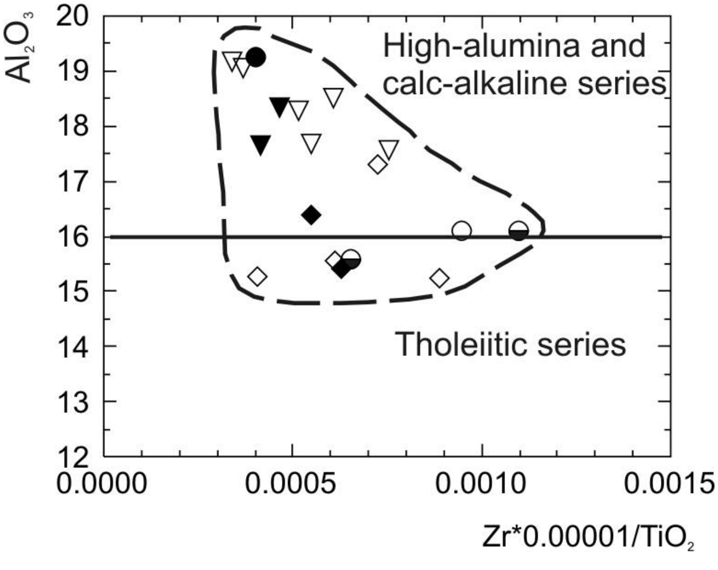

Fig. 12. High-alumina and tholeiitic serial demarcation in the plot Al_2O_3 *vs.* Zr/TiO_2 (Wilson 1989) only for dykes of basalt and basaltic andesite affiliation. The ratio Zr/TiO_2 is used as an index of the magmatic differentiation in the assigned for certain dykes to the dyke pulses

falling in “tephrite” TAS-field, a weak negative Eu-anomaly is marked. A possible explanation might be variable degrees of plagioclase fractionation. The lowest degree of enrichment compared to the chondrite values is for the “tephrite” sample of the pulse II, which makes this sample similar to the basic dykes. These peculiarities of the sample demonstrate that the high alkalis in this sample are not its primary features, but a result of the superimposed alterations. The patterns for the pulse II are remarkably coordinated and similar, which indicate relatively small degree of partial melting in the magma source, leading to preferential enrichment of the *LREE* in the melt and thus to the observed slope. The fractionation within the magmas of the pulse II is responsible for the slight differences in the patterns of the andesite and dacite.

The chondrite-normalized *REE* patterns for representative samples from the pulse III are shown in Fig. 13B. Compared to the pulses I and II, the patterns are a bit weaker fractionated in their *LREE* relative to *HREE* distributions and the fractionated factor ranges 2.5-3.5. The consecutive increasing of the normalized values in the sequence basaltic andesite-andesite-rhyolite supports the magma differentiation in this pulse. The rhyolite dykes display higher enrichment levels for the *LREE* part of the pattern (the ratio $(La/Sm)_N$ is larger than in the other dyke varieties) and a slight negative Eu-anomaly.

All patterns of the samples from the pulse IV are remarkably consistent and show weak positive Eu-anomalies. The fractionation of the patterns is directed only to the increase of the total alkalis in the sequence basalt-“hawaiite”-“shoshonite”-“potassium trachybasalt” as a

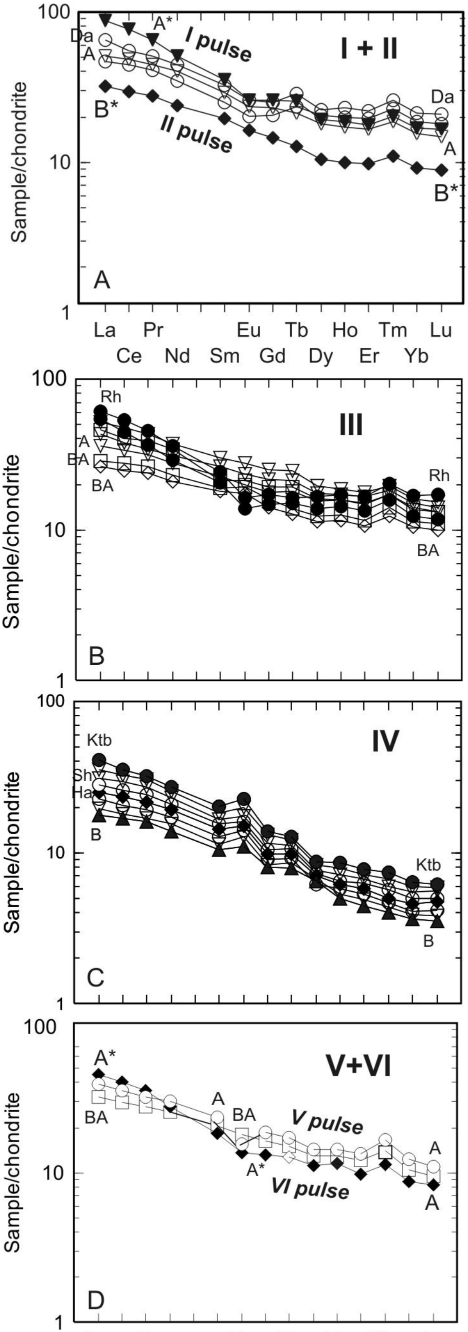

Fig. 13. Selected chondrite-normalized *REE* patterns for representative dykes from different dyke pulses. Rock abbreviations: (B) basalt, (BA) basaltic andesite, (A) andesite, (Da) dacite, (Rh) rhyolite, (B*) strongly altered basalt falling in TAS-diagram in “tephrite” field, (A*) altered andesite as “latite”. The patterns for IV pulse are indicated with the TAS-nomenclature to show the influence of alterations: (Ha) “hawaiite”, (Sh) “shoshonite” and (Ktb) “K-trachybasalt”

result of the degree of alteration. Accumulated plagioclase might be responsible for the slight positive Eu-anomaly observed in these mostly basaltic dykes (Fig. 13C) having very high quantity of plagioclase phenocrysts. Similar effect might be realized due to the amphibole fractionation, but than the influence of such a process should be a scarcely perceptible. The total lack of negative Eu-anomaly in all samples from the pulse IV indicates that plagioclase separation before emplacement of the dykes has been almost impossible. In spite of the fact that the enrichment compared to the chondrite is smaller (between 16 and 30 times for *LREE* and between 3.5 and 6.1 times for *HREE*), the fractionation factor is around 5 to 6 and the slope of the curves is one of the steepest out of all dykes in Hurd Peninsula. A possible explanation might be variable degrees of orthopyroxene fractionation and not necessarily different magma sources or degrees of partial melting, because such conditions would obviously affect all dykes from the respective pulses and not only selected ones as those of the intrusive pulse IV.

The displayed patterns of the chondrite-normalized *REE* distributions of the pulses V and VI shown in Fig. 13D are typical for their weak fractionation of *LREE* over HREE. The fractionation factor is 3.1-3.2 for the samples of the intrusive pulse V and 5.2 for the single sample referred to the pulse VI. The observed slope of the last sample is rather steep also in the *LREE* half of the pattern: $(La/Sm)_N = 4.1$ but not 2.7-3.7 as it was in the samples from the pulse V. These differences are not a result of fractional differentiation. The slight positive Tm-anomaly is outlined in all samples referred to the last two pulses. It is a characteristic feature, but for the time being no acceptable geochemical interpretation is valid for it.

MORB-normalized distributions

Compared to MORB the most distinctive feature of the dykes from Hurd Peninsula is that they are depleted in compatible elements and moderately enriched in incompatible elements (Fig. 14). The elements from the left side of the diagrammes reflect dominantly the effects of the slab-derived components, while the ones on the right side of the patterns might be related to melting and fractionation processes (Elliot 2003). In general sense, this implies a clear island-arc setting. N-MORB-normalized trace element patterns of incompatible elements for some of the dated representatives of the here defined intrusive pulses (Fig. 14) are used to discuss the magma-source characteristics.

Selected samples from the pulses I and II are present in Fig. 14A. Obviously the strong LILE-enrichment of K, Rb, Ba and Th is typical for the subduction zones. These elements are known to be enriched the most in the sediments, but also they are the easiest soluble in the fluids. Therefore, the mantle magma source has been enriched by components introduced from the subduction slab, no matter if fluids or sediments were responsible for the result. The sediment input into the magma source might be suggested by the presence of a strong positive anomaly for Pb in the primitive mantle-normalized plots, (not shown here), as well as the positive anomalies for Ce and Sm. But we must have in mind that Pb also could migrate, according to the model of Chovel et al. (1995), from the interior of the oceanic crust to the surface during the hydrothermal alteration enough effectively. Typical peculiarity of the trace element signatures in the subduction zones are the negative anomalies for Nb and Ta (Nb-Ta "troughs" and thus high Th/Nb ratios expressed in arc magmas spidergrammes). These peculiarities are diagnostic for supra-subduction setting. The depletion of HFSE relative to *REE* in the mantle wedge before the melting is probably a result of *LREE*-enriched influx into the peridotite, which had had chemistry close to the N-MORB before subduction. The lower Ti and Zr concentrations compared to the average N-MORB might be due to the residual Ti- and Zr-bearing phases, but also could be a result of different fractionation histories. The both elements in

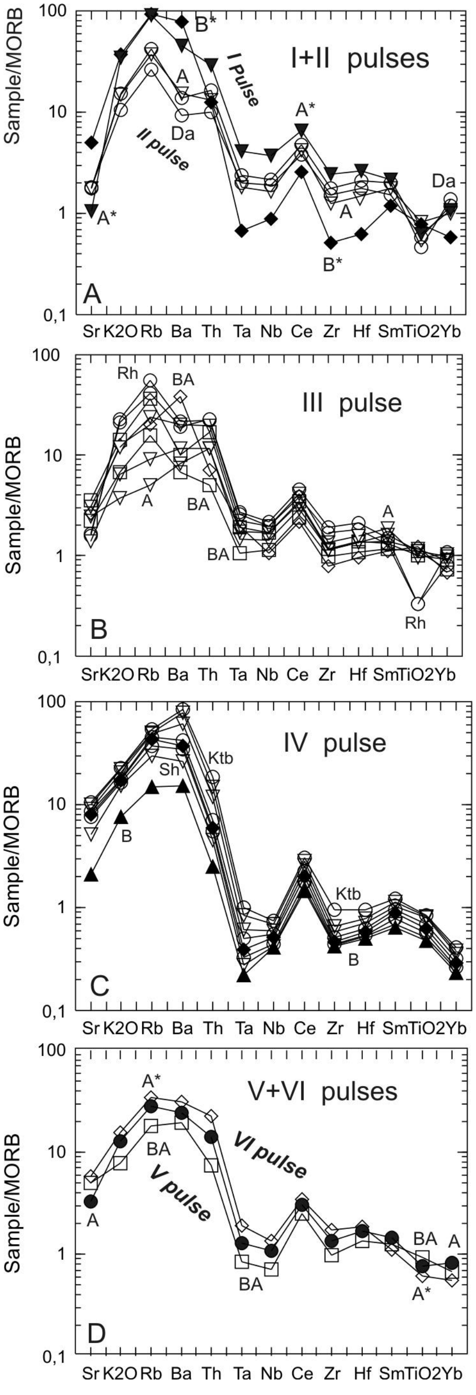

Fig. 14. Selected MORB-normalized trace element patterns for representative dyke samples of different dyke pulses, arranged according to their consecutive younger age. The abbreviations for the rock nomenclature are the same as in the Fig. 13

samples with contents of MgO<6 wt% could be eliminated by fractionation of Ti-magnetite, zircon, rutile and amphibole (as the case is in the pulses I and II). Geochemical prove for amphibole fractionation and up to certain degree of augite is the established moderate positive correlation between the differentiation indexes (SiO_2, MgO) and the ratio Zr/Sm (not shown here). Substantial distinction of the sample belonging to the pulse I is its relatively higher degree of *LILE*-enrichment and the very slight and hardly perceivable negative Ba-anomaly, related to the very high amount of the alkalies in the altered andesite. All the rest samples from the pulse II display nearly identical patterns and only the "tephrite" (altered basalt) differs a little for its too low Sr values, the highest K, Rb and Ba and the strongest depletion of HFSE. These differences are due to a great extent to the alteration of the sample and the hydromagmatophile elements influx in its composition.

MORB-normalized models of representative samples from the pulse III are like those of the pulses I and II (Fig. 14B). The larger extent of the internal differentiation in the pulse III is outlined with the gradually elevation of the normalized amounts of K, Rb, Ba and Th in the sequence: basaltic basaltic andesite-andesite-rhyolite. The patterns are internally consistent and only in their *LILE*-halves they are more dispersed. Generally *LILE*-enrichment is bits more moderate than in the dykes from the pulses I and II. The positive peak at Sm is weaker pronounced. The negative Ti-anomaly is a lot better expressed in the rhyolite sample.

The selected samples from the pulse IV (Fig. 14C) display the typical for the basic rocks MORB-normalized patterns, but on the background of their affinities to the subduction-related magmatism they show also some differences. The lack of the negative Ba-anomaly is one of the most characteristic distinctions. The strongest positive anomalies in the patterns are just at the position of Ba. The feldspar accumulation in these dykes evidently is reflected in this peculiarity. The negative Nb- and Ta-anomalies are located much lower bellow the N-MORB values and a slight negative anomaly is formed on the place of Ti instead the usual positive Ti-anomalies. The internal differentiation within the pulse is well expressed in the sequence: basalt-"shoshonite"-"potassium trahybasalt" which obviously depends also on the degree of alteration.

The *LILE*-enrichment in the samples from the pulses V and VI (Fig.14D) is a little more moderate, but the patterns are not very much unlike between them here as well. The strongest enrichment in these patterns is at Rb position. The negative trough at the position of Ba is not established similarly here. The positive Ce-anomaly is preserved, but the normalized values of Ti are not outlined relative to the neighbouring in the spidergrammes values.

Y is checked for immobility, because it may be mobile during the alterations (McLean & Barrett 1993). It is plotted between Dy and Ho due to the similarity of theirs ion radiuses on a normalized to primitive mantle diagramme (here not shown). Actually in our case of the dykes from Hurd Peninsula no any Y-anomalies in such diagramme are noted, meaning that Y preserves its immobile behaviour during the alteration and therefore, the element is a reliable geochemical indicator for the petrogenetic history of Hurd Peninsula.

Fractionation

Negative correlations between SiO_2 and MgO, CaO, TiO_2, FeO, Cr, Co, Ni and V, as well as the positive correlation between CaO and MgO in the dyke set imply that dyke compositions have been under olivine/orthopyroxene control, down to ≈ 7 wt.% MgO of the magmas. At this point a Ca-rich phase, either augite or plagioclase began to fractionate. CaO/Al_2O_3 ratios correlate positively with the $Mg^{\#}$ ratio; hence substantial crystal fractionation is required to explain the characteristics of the basic dykes. Cr and Ni abundances in the dykes are too low to had been in equilibrium in a mantle source. Thus, no samples appear to represent a primary mantle-derived magma and all are fractionated to different degree, so it is important in later discussion of mantle sources to select element ratios not affected by crystal fractionation processes. The evolved nature of the most primitive of the dykes and the simple negative correlation of $Mg^{\#}$ ratio with incompatible element enrichment imply that these compositional changes are a result of crystal differentiation, not of variable degree of partial melting.

The general positive correlations between Na_2O, K_2O, Rb, Zr and Nb vs SiO_2 demonstrate an evolution from basic to intermediate magma and common chemical affinity of the different dykes. As we have already demonstrated, the range of the chemical evolution of the dykes from the individual pulses is different. The negative correlations of Ti and V with Zr and with the ratio FeOt/MgO and the invariably low TiO_2 whereas Al_2O_3 is rather high are typical characteristics of many arc rocks.

The most reliable arguments for the magma source characteristics came out of the geochemistry of the basic dykes, but a comparison of their spidergrammes with those of the most acid and evolved dykes provide information about the differentiation within the magmas. Such a comparison is justified, but excluding the Eu-anomalies and the highest normalized concentrations in the evolved samples, the chondrite-normalized *REE* patterns are almost similar. This fact rejects the possibility these dykes to represent material generated through melting of the continental crust beneath the South Shetland Islands. The *REE* pattern then would be completely different if the acid dykes were derived from crust melting. This admission is supported strongly by the almost identical $^{87}Sr/^{86}Sr$ ratios

(Kraus et al. 2007) between the acid and the basic dykes in the archipelago. The Th and U concentrations are nearly 5 to 8 times higher in the acid dykes, which follows from the incompatible behaviour of these elements during the magma differentiation. A much more interesting is the behaviour of Nb and Ta. As Nb displays the well-known negative anomaly, typical for the subduction zones, the negative Ta-anomaly wanders significantly and the ratios $(Nb/Ta)_N$ are either >1 or <1. This observation shows that in the acid dykes both elements have no behaviour of "geochemical twins", as it is in the basic dykes. Than the existence of a hypothetical process leading to fractionation of the both HFS elements in the strong evolved systems is justified.

The negative anomalies for Sr, Ti and P (the last element is omitted in the present variation diagrammes with the purpose they to be made simplified) are one of the most characteristic features of the MORB-normalized diagrammes of the dyke samples studied. All these peculiarities are related to crystal fractionation of plagioclase, apatite and ilmenite/titanite. This conclusion is supported by the observed mineral composition of the dykes – the plagioclases being the principal rock-forming phenocrysts in almost all basic and intermediate dykes and apatite is an often met accessory mineral in the ground mass of the dykes. However, apatite and ilmenite are of no importance and they are absent in the Si-rich dykes.

Melting degree and differentiation

The Yb enrichment relative to primitive mantle displays the degree of partial melting if is applied only to the basic members of a rock suite, and may serve as a differentiation index if applied also to the evolved members of this suite. In order to express the genetic distinctions between the analyzed geochemically and dated dyke pulses, we draw a plot of Yb_N *vs.* $Mg^\#$ (Fig. 15). Mg-number is insensitive to the partial melting, but can serves as an index of fractional crystallization. The following conclusions result from the plot: (1) the pulses I, II and III have experienced significant fractional crystallization as indicated by their low $Mg^\#$. These dykes have been intruded over a longer time period permitting wider range of differentiation; (2) The pulse IV distinguished by its higher $Mg^\#$ value experienced shorter storage time in its magma chamber and thus it represents a less evolved magma. The lower

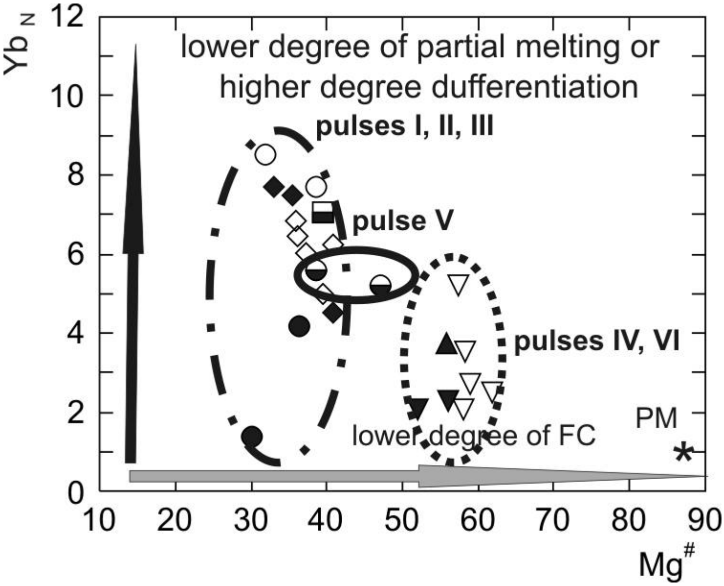

Fig. 15. Yb_N *vs.* $Mg^\#$ plot for selected different dyke pulses on Hurd Peninsula. Yb normalized to primitive mantle (McDonough & Sun 1995) is used as an index of crystal differentiation. Symbols for dyke pulses correspond to those in Fig. 4. The average value of the primitive mantle (PM) is after McDonough & Sun (1995)

degree of fractionation for these dykes is also confirmed by their lower Yb_N values, high Ni (up to 100 ppm) and Cr (up to 170 ppm) abundances. Meanwhile the dykes from the pulse IV bear the traces of considerable fluid influx to the mantle source, as it was shown from their very high Ba/Th ratios; (3) the dykes from the pulse V have had intermediate stories judging from their positions between the Yb_N and $Mg^{\#}$ values.

Discernable geochemical features of the different dyke pulses are outlined also in Fig. 16 comparing the degree of alkalinity expressed as the ratio Nb/Y against the fractionation index $Mg^{\#}$. Two groups of dykes are delineated again. The first one includes the dyke pulses from the most differentiated dykes with lowest $Mg^{\#}$ ratios (I, II and III). The highest degree of alkalinity of the pulse I might be a result of stronger crustal contamination as indicated by its position directed closer to the average upper continental crust (UCC), while the pulse II is in lowest position and thus least contaminated. Probably the dykes from the pulse II might have had shorter residence time in the shallow level magma chamber in contrast to the ones from the pulse I. Weak crustal contamination is also suggested for the dykes of the pulse V, which are also amongst the dykes with intermediate degree of differentiation. The second group of samples covers the dyke pulses VI and IV having the highest $Mg^{\#}$, but differing between them by the degree of their alkalinity or of their crustal contamination.

The melting degree of the different dyke pulses might be estimated using the quantitative approach proposed by Pearce & Parkinson (1993) and demonstrated in Fig. 17 on the constructed Nb *vs.* Yb plot. To avoid the differentiation influence on the results only the most primitive samples (MgO> 6 wt. %) are examined. Most of them are from the pulse IV, but the pulses II, III and VI are also presented. The mantle source was obviously enriched by the subduction process and the deduced melting degrees range between 15 and 40 %.

The systematic covariation of Sr, Ba and Ca elements proposed by Onuma (1981) for meteorites and applied by Zheng & Liu (1991) for Cenozoic volcanic rocks from King George Island seems to be related to their magma generation and fractionation history. An attempt to use this covariation as an indicator of the genesis of dated dykes from Hurd

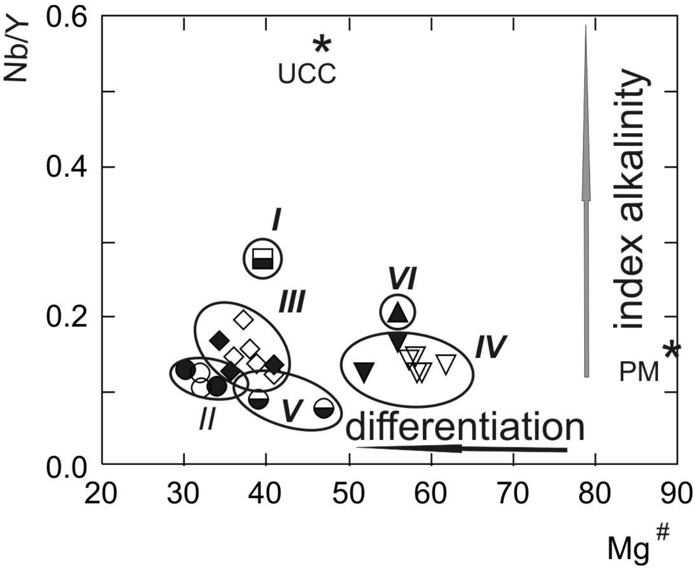

Fig. 16. $Mg^{\#}$ *vs.* Nb/Y ratio to demonstrate distinct geochemical properties of the individual intrusive dyke pulses on Hurd Peninsula by degree of differentiation and alkalinity. Primitive mantle value (PM) is from McDonough & Sun (1995) and upper continental crust (UCC) one is from Rudnick & Gao (2003)

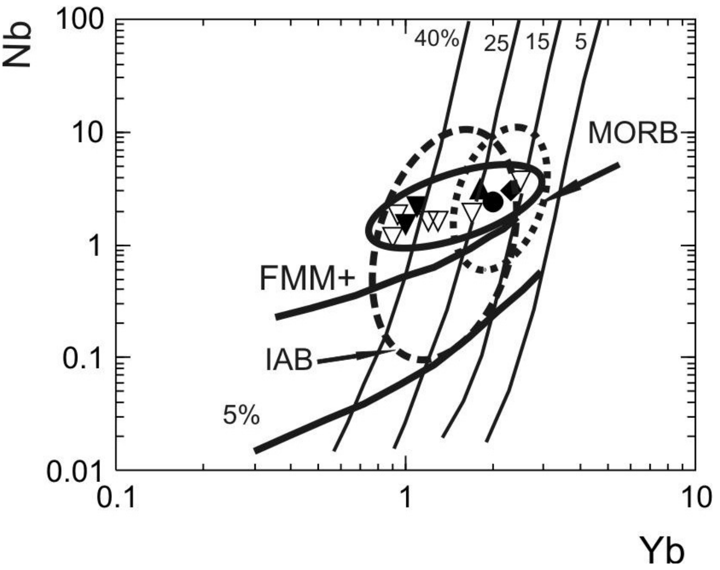

Fig. 17. Nb *vs*. Yb plot for primitive samples (MgO > 6 wt. %) of second, third, forth and sixth dyke pulses to estimate degree of melting. Theoretical contours for degree of melting, degree of mantle depletion (below FMM+ line), MORB and continental arcs fields are from Pearce & Parkinson (1993). The solid symbols are for dated dykes and the open ones – for geochemically distinguished dykes. Abbreviations: (MORB) middle ocean ridge basalts, (IAB) island arc basalts, (FMM) fertile MORB mantle

Peninsula is shown in Fig. 18. The partial melting line has been estimated on the basis of melting experiments of a garnet-bearing peridotite mantle with chondritic Sr/Ca and Ba/Ca ratios (Tera et al. 1970; Mysen & Kushiro 1977). Nearly all samples dated as Late Cretaceous and Paleocene dykes (stage 1) plot along the clinopyroxene control line diverging from the partial melting line at 2 %. This suggests evolution of these dykes from basalts (sample with serial number 5, Table 2 having the closest to the primary magma

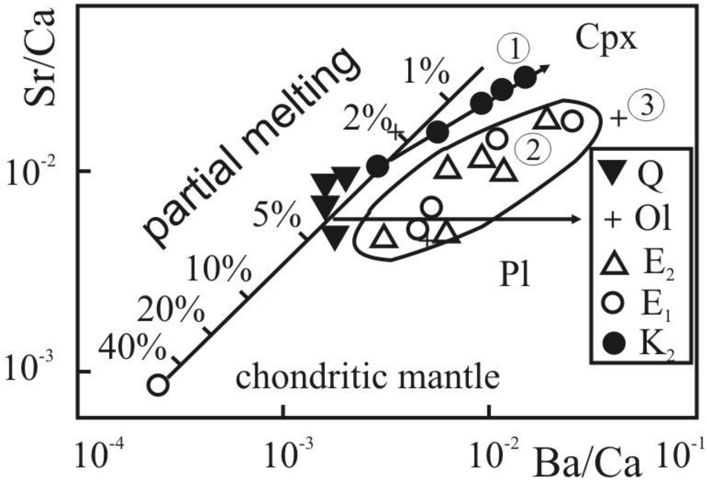

Fig. 18. Sr/Ca *vs*. Ba/Ca systematic covariation diagram (Onuma 1981). Chondritic mantle is from Tera et al. (1970). Fractional crystallization vectors: (CPx) clinopyroxene, (Pl) plagioclase. Ages: (1) Late Cretaceous-Paleocene, (2) Ypressian, (3) Lutetian (4) Oligocene (5) Quaternary to Recent basalts

characteristics) through intermediate varieties controlled by crystallization of clinopyroxene. Dykes of Eocene age (stage 2) delineate an elongated field intersecting the partial melting line at higher degrees of melting (up to nearly 40 %). The partial magma of these dykes has been probably derived by certain amount of plagioclase fractionation of the primary magma. The evolution trend of dated dykes of Eocene age is directed from basalts and basaltic andesites through andesite, mugearite, shoshonite to latite. This trend was controlled by crystallization of clinopyroxene and plagioclase. Olivine and magnetite crystallization could not be visualized on this diagramme as these minerals do not accept Ca, Ba and Sr and hence do not change the Sr/Ca and Ba/Ca ratios of the parental magmas. But compatible trace element variations give an indication of the crystal fractionation process (for example Ni and Cr abundances systematically decrease as $Mg^{\#}$ decreases), consistent with the fractionation of olivine or olivine + clinopyroxene from originally more mafic magma.

Mantle wedge

The mantle source beneath the South Shetland Islands is characterized by the absence of residual garnet as indicated by the *LREE* patterns and the missing of *Y* anomaly.

The abundances and ratios of the HFSE have been used recently to trace the original composition of the mantle wedge prior to its enrichment (Eggins et al. 1997; Elliot et al. 1997; Plank & White 1995). These elements are less abundant in sediments and that is why they produce the least enrichment in the wedge by sediment input (Woodhand et al. 1993). Moreover, they are not readily mobilized and transported by aqueous fluids from the oceanic crust (Tatsumi et al. 1986; Wilson 1989). The majority of the inter-element ratios of HFSE cover nearly same ranges for the dykes of different age. For example, the total range in Zr/Nb ratio in all magmatic stages for the most primitive compositions is not very much unlike – 18-60. The almost common extent of the ratios like Zr/Nb and Ti/Nb for all studied dykes, independently of their age, supports for their common source, which did not change essentially its HFSE-signatures.

Nb and Ta are especially important amongst HFSE. Being with the highest incompatibility these elements should be most affected by prior mantle depletion under usual mantle conditions. Their ratios in contrast to ratios of the less compatible HFSE are weakly influenced by variations in melting and fractional crystallization. However, experimentally determined distribution coefficients suggest that Nb is slightly more incompatible in common mantle minerals than Ta (Green et al. 1989) and therefore melting should reduce the Nb concentration and the ratio Nb/Ta in the residue (Elliott 2003).

An expressive tracer for depletion of the mantle source is the ratio Nb/Ta. The lower than N-MORB and primitive mantle values ratio is of importance because it is usually considered as a measure of the source depletion prior to arc magma genesis (Elliott 2003). The ratios Nb/Ta displayed in Fig. 19 for basalts and basaltic andesites only are in most cases really lower than in the average primitive mantle and even to the lesser degree than N-MORB, thus giving strong evidence for source depletion and indicating a heterogeneous mantle wedge beneath South Shetland Islands. The ratio $(La/Sm)_N$ reflects the additions to the source during the arc genesis.

In order to illustrate the changing degree of source enrichment (K_2O/MgO ratio) and variability of incompatible element ratios (K_2O/TiO_2) with emplacement age of the dykes we constructed Fig. 20 compiled all available our data with the ones of Kraus et al. (2007). TiO_2 and MgO were chosen as one of the most immobile components and K_2O as a sensitive to contamination processes component. No obvious correlation was established when we put all set of the dated dykes in the figure. Interesting is that when the subset of the heavily altered and strong evolved dykes was

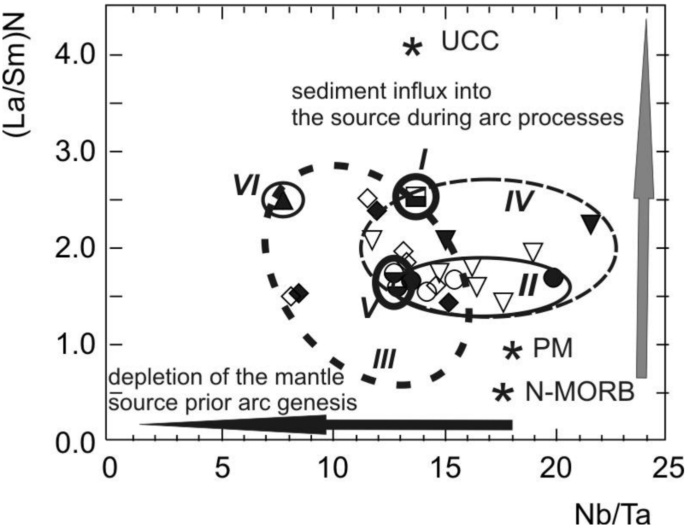

Fig. 19. Nb/Ta ratio *vs.* $(La/Sm)_N$ ratio to visualize the sediment influx and a depleted in HFSE mantle source for selected different dyke pulses on Hurd Peninsula. The values of upper continental crust (UCC), primitive mantle (PM) and N-MORB are as in Fig. 10

separated, the relatively more primitive dykes formed a clear trend pointing to the higher ratios with time for the different magmatic dyke stages. The same regularity is notable for the plot K_2O/MgO *vs.* the age of the dykes (Fig. 20B). Possible explanation is that the younger the stage is, the more enriched in *LILE* is its magma source. However dangerous it may be to use an element like K, which demonstrated well its mobile behaviour, this trend of the fresh and primitive dyke samples of increasing its *LILE* with time could be significant. Nevertheless, the same similar systematic increase of the range of Zr/Y ratio to the younger dykes (Fig. 20C) does not depend on the alterations of the samples due to the immobile behaviour of the both elements. The magmatic record of subduction beneath Antarctic Peninsula and beneath South Shetland Islands extends far back as the Jurassic time. The geophysical evidence shows that oceanic crust was being generated at spreading ridges in the South Pacific from at least Cretaceous (Pankhurst 1982; Herron & Tucholke 1976; Rex 1976). *LILE* and HFS-element enriched fluids many times influenced the subcontinental mantle. The long subduction history of the source region certainly contributed for enrichment of the source more heavily in the younger in age dykes.

Plate-derived components

The slab-derived components contributing to arc genesis beneath South Shetland Islands includes: (1) subducted sediments and (2) fluids from the altered oceanic crust (Class et al. 2000; Elliott 2003; Elliott et al. 1997; Hawkesworth et al. 1997; Turner et al. 1996, 1997, 2000; Turner & Hawkesworth 1997 etc.). The contributors to the magma source might be identified by trace element and isotopic systematic. We apply here the first approach.

The sediment input. Enrichment of *LREE* relative to *HREE* in the *REE* patterns of the dykes is the first hint to possible sediment input in their magma source, but if it is combined with high Th abundances. High ratios Th/Ce and low U/Th, as well as the low εNd isotopic values and high Pb isotopic ratios (Kraus et al. 2007) are also typical sediment signatures. The plot of $(La/Sm)_N$ *vs.* Nb/Ta ratios (Fig. 19) constructed for the different dyke pulses is helpful also in the estimation of the relative significance of the sediment input against depletion of the source prior to arc magmas production. The magmas of the pulses I and VI probably carried out the strongest influence of the sediment additions to the source, while the pulses II and V are least contaminated with sediment materials. Meanwhile, the depletion of the magma source has been variable during the generation of the magmas of the dykes. The dyke pulses II, IV and possibly I demonstrate lower depletion degree of their source than the dykes from III, V and VI pulses. The positive correlation between the ratios $(La/Sm)_N$ and Th/Nb in Fig. 21 is also a strong argument for the probable sediment input to the magma source (Plank & Langmuir 1998). The majority of the samples are piled together towards lower values of the ratio Th/Nb, thus suggesting generally lower sediment influx to the source area during early magmatic stages. The almost linear trend does not suggest the upper continental crust (UCC) to play a significant role for the budget of these elements, as UCC does not plot in an end-member position of the trend. The deviations from the correlation (pulses I and III plotted well above the general trend) may indicate an enrichment process induced by fluids rather than sediment influx, because Th is considered immobile under aqueous conditions. This does not exclude the other possibility – the effect of the fractionation to be partly the likely explanation also. Similar conclusions are achieved by Kraus et al. (2007) for the dykes from the whole South Shetland Islands area.

High sediment input may cause a negative Ce anomaly, but also increasing Th abundances. Thus, a low Ce/Th ratio might reflect a strong sedimentary component. The trend towards lower Ce/Th ratios with the rejuvenation of their age shown in Fig. 22 (Ce/Th *vs.* age) is indicative. It seems that generally the sediment influx to the mantle source got stronger with time, coming out of the lowering the ratios Ce/Th to the younger pulses.

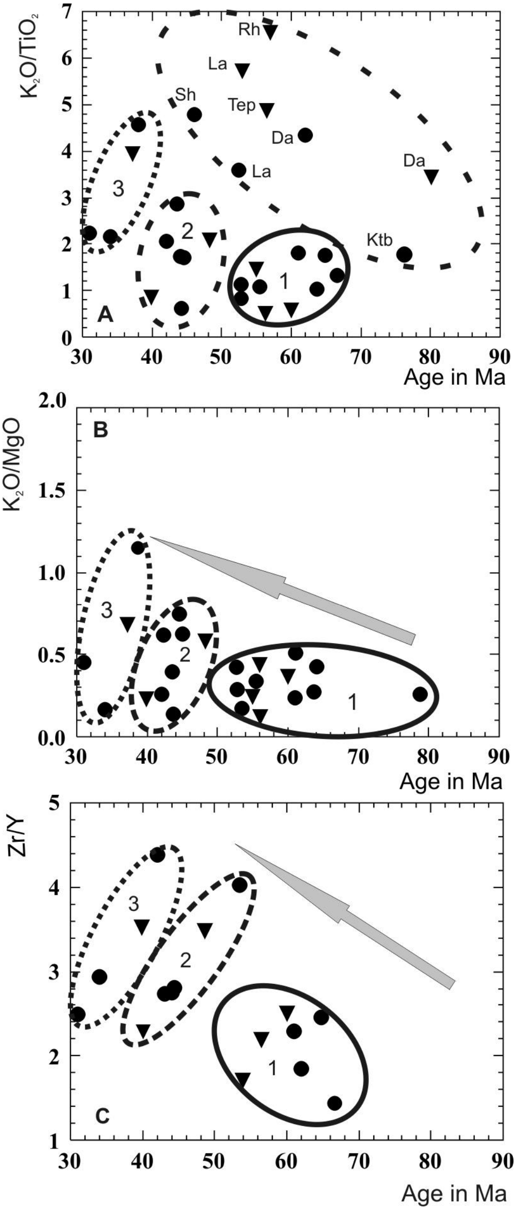

Fig.20. Illustration of the variability of incompatible element ratios with age for the dated dykes in Hurd Peninsula. A) K_2O/TiO_2 *vs.* age in Ma plot. The evolved and transitional in alkalinity altered dykes are confined within the upper field: (Rh) "rhyolite", (La) "latite", (Sh) "shoshonite", (Tep) "tephrite", (Da) "dacite", (Ktb) "potassium trachybasalt". Magmatic stages 1, 2 and 3 are outlined for the basic primitive samples only. B) K_2O/MgO *vs.* age in Ma plot with the fields of the magmatic stages. C) Zr/Y *vs.* age plot. Symbols: solid circles – this contribution, solid triangles – data from Kraus et al. (2007)

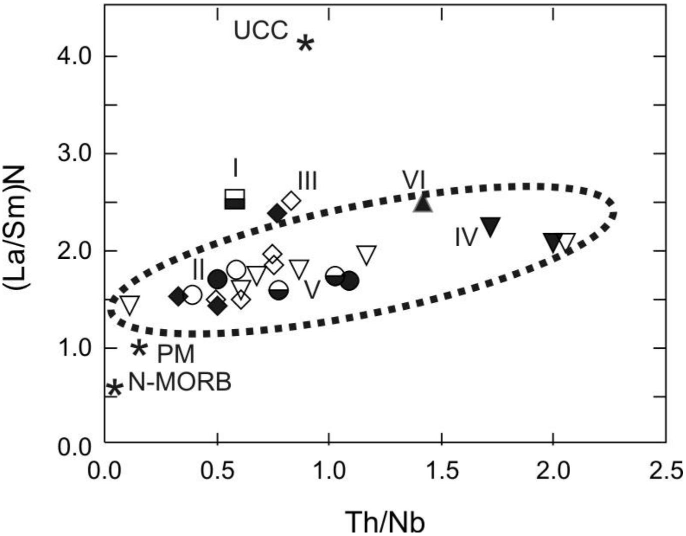

Fig. 21. Positive correlation between the ratios $(La/Sm)_N$ and Th/Nb for basalts and basaltic andesites of the selected dykes from Hurd Peninsula. *LREE* ratio normalized to primitive mantle (PM) values from McDonough & Sun (1995), N-MORB value from Sun & McDonough (1989), upper continental crust value from Rudnick & Gao (2003). Symbols as in Fig. 4

Fluids influx. A useful method to discriminate between the different components transferred from the subducting plate to the mantle wedge is plotting the ratios $(La/Sm)_N$ *vs.* Ba/Th (Fig. 23). High relative Ba abundances (e.g. Ba/Th) can be attributed to fluids derived from the altered oceanic crust (Elliot 2003; Turner et al. 2000; Tatsumi & Eggins, 1995). The reason is that Th is essentially immobile, while Ba as *LILE* is highly mobile in aqueous fluids. In contrast, the sediment involvement may cause relative depletion of Ba of the melt, because Ba would be retained in residual biotite (Nichols et al. 1994) and therefore, the strong sediment input is unlikely to be responsible for Ba enrichment. So that, increased Ba/Th ratios suggests enrichment induced from the fluids derived from the

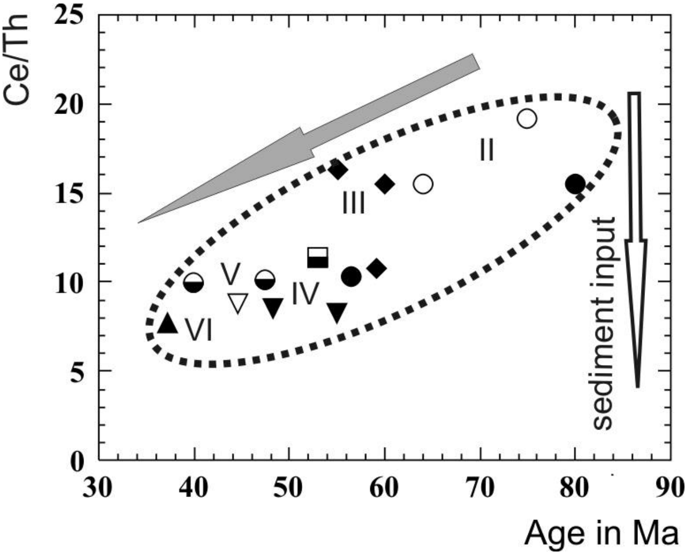

Fig. 22. Negative correlation (shaded arrow) between the decrease of the ages and Ce/Th ratio suggesting increasing sediment input with time for dykes in Hurd Peninsula. Symbols as in Fig. 4

subducting oceanic slab, especially when they are accompanied by low ratios La/Sm. To avoid the influence of the differentiation only relatively primitive dykes were plotted (basalts and basaltic andesites) and the evolved dykes were omitted. The assimilation of continental crust could also be capable to raise Ba abundances, but at the same time would increase Th as well, thus such contamination would not fractionate Ba and Th to explain the elevated Ba/Th ratios. The plot in Fig. 23 indicates a stronger fluid-induced component for the dykes of the pulses II, III and IV and clearly sediment additions in the samples from the pulses I, V and VI, located on the mixing line between the end-members N-MORB and NASC (North American Shale Composite after Gromet et al. 1984). An alternative interpretation of the high fractionated Ba/Th ratios in the dykes from the pulses II, III and IV is the addition of Ba by variable hydrothermal alterations on these samples. Actually, the located in uppermost position on the plot along the component Ba/Th samples are indeed the highest altered representatives of the dykes. Th is insoluble at least in oxidizing conditions and consequently would not be mobilized under such conditions (Turner & Hawkesworth 1997). The discrimination between the both alternative explanations is difficult to be done by the available data.

Hawkesworth et al. (1997) postulated that relative U-enrichment should be realized by fluids, leading to elevated U/Th ratios. The plot of U/Th *vs.* Th for dykes from Hurd Peninsula (Fig. 24), where only basalts and basaltic andesites are displayed, shows that hardly the fluids were only responsible for their variations. The points plotted well bellow N-MORB level indicates again a depleted prior to arc genesis mantle source for their magmas. The observed pattern may be explained either by a contribution of subducted sediments with a relatively low U/Th ratios, or by the availability of a mantle source depleted in U. Crystal contamination is also a likely additional explanation, especially for the earlier dyke magmatic stages, because crustal materials have low U/Th ratios.

The ratio Ce/Pb almost reflects the composition of the magma source and it is usually unaffected by partial melting and differentiation processes at shallow levels (Hofmann et al. 1986; Miller et al. 1997). The generally low Ce/Pb ratios in the arc magmas (<10) are due to the preferential transfer of Pb in relation to Ce from the subducting plate into the mantle wedge (Miller et al. 1987). The plot

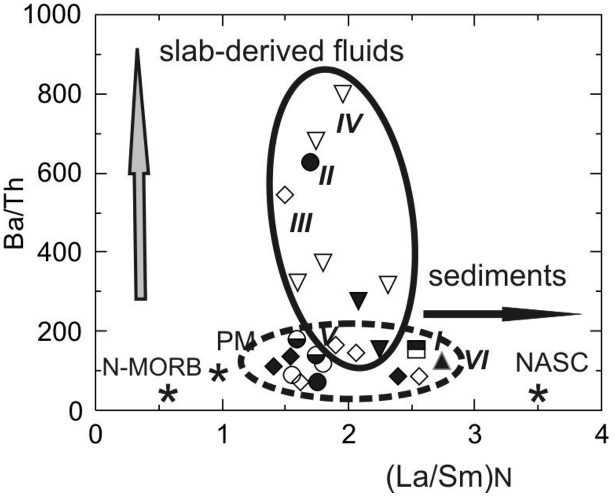

Fig. 23. Ba/Th *vs.* $(La/Sm)_N$ plot to discriminate between slab-derived components (fluid induced and sedimentary input) to the dyke sources for selected representative samples. N-MORB value from Sun & McDonough (1989), North American Shale Composite (NASC) values from Gromet et al. (1984). Normalization of the *LREE* ratio to primitive mantle from McDonough & Sun (1995). Symbols as in Fig. 4

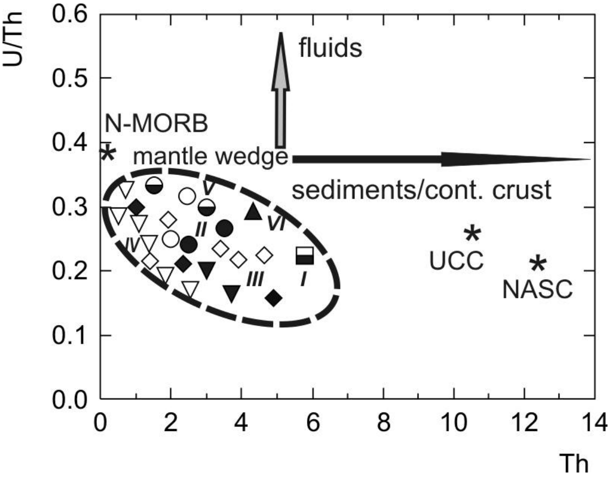

Fig. 24. Th *vs.* U/Th ratios to discriminate between sedimentary/or crust derived components and slab derived fluids for selected dykes from Hurd Peninsula. Only basic dykes are plotted. North American Shale Composite from Gromet et al. (1984). The other symbols are as in Fig. 4 and Fig. 23

in Fig. 25 correlates the ratios Ce/Pb and Ba/Th in the dykes from the different intrusive pulses from Hurd Peninsula. The observed low ratios Ba/Th and high Ce/Pb for the dyke of the pulse I are consistent with unusually low influx of slab-derived fluids to its mantle source. The dykes from the pulse III are the strongest differentiated along the ratio Ce/Pb, but having the lowest Ba/Th ratios thus they are the least influenced by the fluids and owing to their longer stay in the shallow chambers are differentiated wider. The heterogeneous mantle source for the dykes of pulse III is another possible explanation. The strongest influence of the slab-derived fluids was supposed again for the dykes of the intrusive pulse IV, as they show wide range of the ratio Ba/Th.

Crustal contamination

A distinct discrimination between sediment influx and crustal contamination to the magma

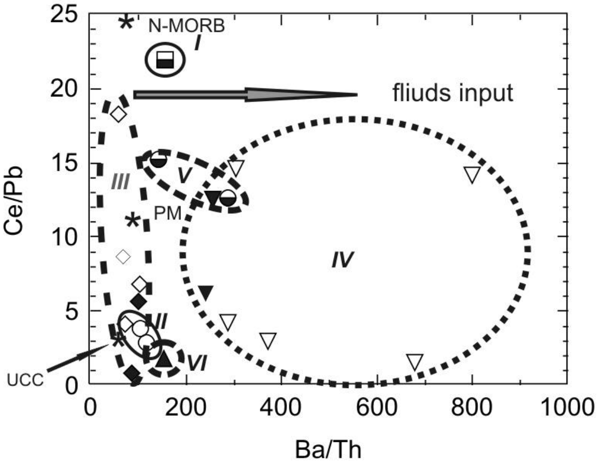

Fig. 25. Ce/Nb *vs.* Ba/Th ratios plot to illustrate the different degrees of fluid influx and the specific geochemical features of the separated dyke pulses in Hurd Peninsula. N-MORB values, primitive mantle values and dyke symbols as in Fig. 4 and Fig. 10

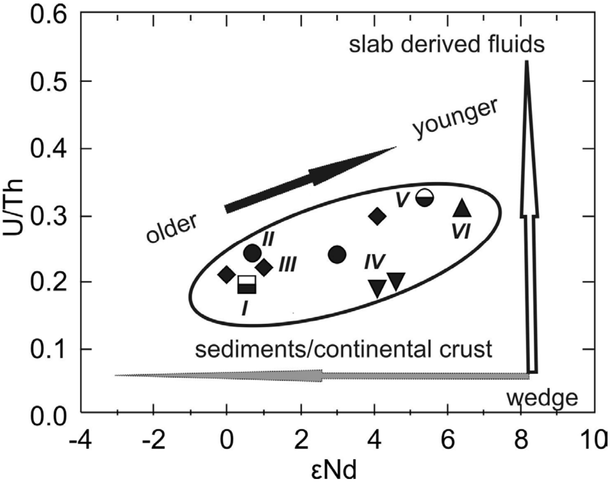

Fig. 26. εNd *vs*. U/Th ratio plot to distinguish between the role of sedimentary/or crust derived components in the genesis of dykes from Hurd Peninsula. The Roman numerals are for different dyke pulses. Symbols as in Fig. 4. Nd isotope data from Kraus et al. (2007). Symbols as in Fig. 4

source of the dykes is difficult in active continental margins settings. Crustal contribution is suggested from the Fig. 24 (U/Th *vs*. Th), but not distinguished clearly from the sedimentary one. Crustal influence on Hurd Peninsula area is assumed also from Sr, Nd isotope data, but similarly is not unequivocal. The plot of U/Th ratio *vs*. εNd in Fig. 26, constructed using the original data of Kraus et al. (2007) in a bit different way, shows clearly that the most contaminated dykes are the oldest intrusive pulses having the lowest εNd values. Consequently, the degree of crustal contamination gradually decreases with time. What is interesting is that a positive correlation between the εNd and $Mg^{\#}$ was proved by Kraus et al. (2007) and confirmed by our data as well (Fig. 27). This result emphasizes the fact that most contaminated dykes from the oldest magmatic stages are at the same time the most differentiated. The interpretation that crustal contamination usually occurs during shallow level differentiation seems logical and it explains why the most differentiated dyke

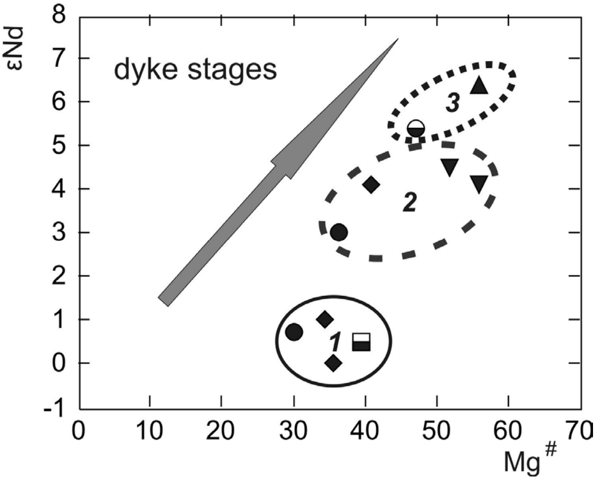

Fig. 27. Crustal contamination as reflected by the correlation of the Nd isotope data with the $Mg^{\#}$ for representative dykes from different dyke pulses in Hurd Peninsula. Nd data from Kraus et al. (2007)

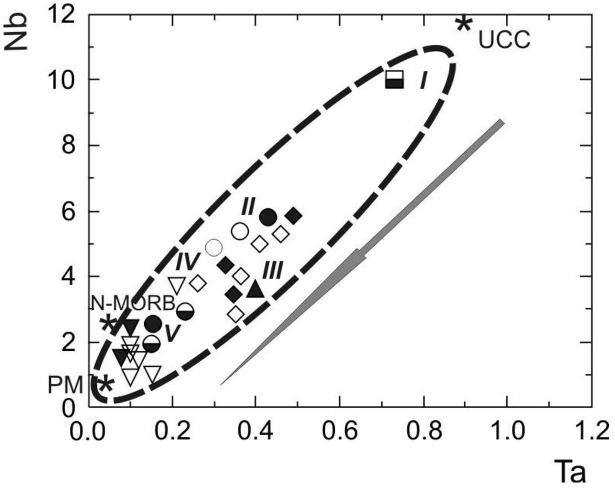

Fig. 28. Nb *vs.* Ta correlation for selected dykes from different dyke pulses in Hurd Peninsula to show mixing between the end-members upper continental crust (UCC) and primitive mantle (PM) and N-MORB. Symbols and bibliographic sources of the reference values as in Fig. 4 and Fig. 10

pulses are the most contaminated. Thus, in the initial stages of the evolution of the young immature arc the still unstretched continental crust is impervious to the rising magmas and the storage magma times at shallow level chambers are longer. The increasingly stretching of the crust let the melts to rise more easily and their storage times at the shallow magma chambers are shorter. The plot of εNd *vs.* the age of the dykes (Zheng et al. 2003; Kraus et al. 2007) illustrates more clearly the conclusion for the gradual decrease of the crustal contamination with time.

The strongly correlated behaviour of Nb and Ta in the dykes from Hurd Peninsula shown in Fig. 28 suggests also mixing between the end-members upper continental crust (UCC) and primitive mantle (PM) and N-MORB and gave another hint for the role of the crustal contamination.

Tectonic discriminations

A tectonic discrimination for the dykes is shown on Fig. 29. On the diagramme after Cabanis & Lecolle (1989) all dated samples fall in the volcanic-arc basalts overlapping with the volcanic-arc tholeiites. Tectonic settings deduced clearly suggest that during magma-generation processes oceanic materials were involved (MORB component of the subducted ridge-crest) as well as a mantle source affected by subduction-related melts and/or fluids (subduction component).

Summary and conclusions

1. The dykes studied are altered in different extent discrediting all TAS-classification nomenclatures. The revised nomenclature of the dykes using immobile trace elements discards the transitional in alkalinity rock varieties and confirms only the following suite of rocks: basalt – basaltic andesite – andesite – dacite – rhyolite as a typical for Hurd Peninsula area. The magmatic serial affinity of the dykes is predominantly tholeiitic with some calc-alkaline series in the later stages of evolution.
2. The dykes are assigned to six dyke pulses, according to their crosscutting relationships and their geochemical features. The already published isotope dating of representative dykes are the basis of integration the dykes into three magmatic stages: (1) 80-55 Ma (dyke pulses I, II and partly III); (2) 48-42 Ma (pulses IV and partly III) and (3) 40-31 (pulses V and VI). These stages correspond perfectly to the restricted range of phenocrysts clinopyroxene composition.

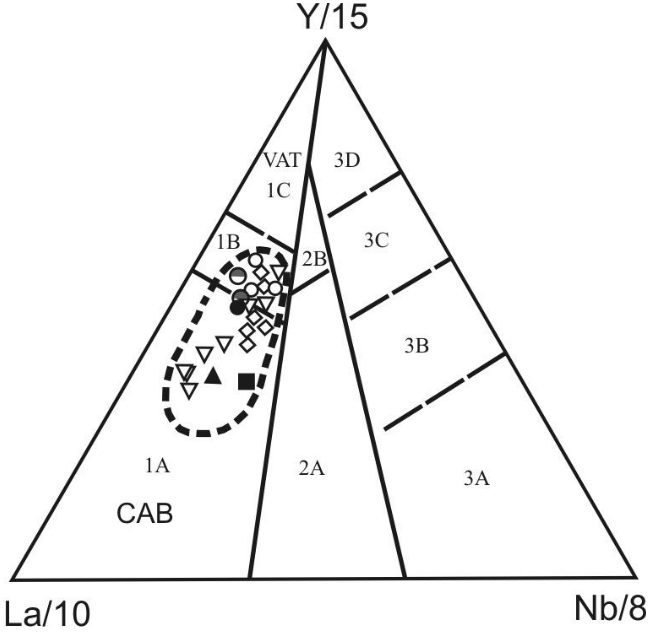

Fig. 29. Tectonic discriminant diagram La-Nb-Y for selected dykes from different dyke pulses in Hurd Peninsula after Cabanis & Lecolle (1989). Settings: 1 – volcanic arc basalts; 1A – calc-alkaline basalts (CAB); 1B – overlap between A and C; 1C – volcanic arc tholeiites (VAT); 2A – continental basalts; 2B – back arc basin basalts; 3A – alkaline basalts from intercontinental rifts; 3B – strongly enriched E-type MORB; 3C – weakly enriched E-MORB; 3D – N-MORB

3. The subduction-related signature of all dykes is confirmed geochemically.

4. The variety of the dyke composition has been controlled by the following geochemical components: (1) The heterogeneity of the mantle wedge; (2) Sedimentary input to the mantle source; (3) Fluids influx from the altered oceanic crust; (3) Crustal contamination to the source; (4) Melting degrees and crystal fractionation of the partial magmas. Each one of these factors was estimated by some geochemical constraints.

5. The mantle source is characterized by the absence of residual garnet, depletion of the ratio Nb/Ta and U before subduction and enrichment of *LILE* during subduction episodes.

6. Substantial crystal fractionation is required to explain the geochemical characteristics of the dykes. The magma evolution of the partial magmas in the different dyke pulses was controlled by fractionation of olivine, clinopyroxene, plagioclase, magnetite, apatite and zircon.

7. Some time-dependant geochemical ratios are revealed. They support a gradual increasing of the basicity and alkalinity of the parental magmas and a tendency of slight increasing of the fluids and sedimentary inputs to the sources, as well as a decreasing of the crustal component with their age rejuvenation.

Acknowledgments: The Contract 685/10.02.2005 with the Ministry of Environment and Water Resources in Bulgaria supported part of this work financially.

References

Cabanis B, Lecolle M (1989) Le diagramme La/10-Y/15-Nb/8: un outil pour la discrimination des series volcaniques et la mise en evidence des processus de melange et/ou de contamination crustale. *Comptes Rendus de l'Academie des Sciences*, Paris, II, **309**, 2023-2029.

Caminos R, Marchese HG, Massabie AC, Morelli JR, Rinaldi CA, Spekermann JP (1973) Geologia del sector noroccidental de la Peninsula Hurd, Isla Livingston, Shetland del Sur, Antartida Argentina. *Contribuciones Cientificas del Instituto Antartico Argentino,* **162**, 32 p.

Chauvel C, Goldstein SL, Hofmann AW (1995) Hydration and dehydration of oceanic crust controls Pb evolution in the mantle. *Chemical Geology*, **126**, 65-75.

Class C, Miller DM, Goldstein SL, Langmuir CH (2000) Distinguishing melt and fluid subduction components in Umnak Volcanics, Aleutian Arc. *Geochemistry Geophysics Geosystems*, **1**, 1999, GC000010.

Dabovski C, Harkovska A, Kamenov BK, Mavrudchiev B, Stanisheva-Vassileva G, Yanev Y (1991) A geodynamic model of the Alpine magmatism in Bulgaria. *Geologica Balcanica*, **21**, 4, 3-15.

Davies A, Blackburn WH, Brown WR, Ehmann WD (1978) Trace element geochemistry and origin of Late Precambrian: Early Cambrian Catoctin greenstones of the Appalachian Mountains. *Univ. of California at Davies, Davies Calif. Rep.* (unpublished), cited after Schweitzer J, Kröner A (1985).

Eggins SM, Woodland JD, Kinsley LPJ, Mortimer GE, Sylvester P, McCulloch MT, Hergt JM, Handler MR (1997) A simple method for the precise determination of > 40 trace elements in geological samples by ICP-MS using enriched isotope internal standardisation. *Chemical Geology*, **134**, 311-326.

Elliott T (2003) Tracers of the slab. In: Filer J (Ed.): *Inside the Subduction Factory: AGU Geophysical Mon.*, **138**, 23-45.

Elliot T, Plank T, Zindler A, White W, Bourdou B (1997) Element transport from slab to volcanic front at the Mariana arc. *Journal of Geophysical Research*, **102**, 14991-15019.

Floyd PA, Winchester JA (1978) Identification and discrimination of altered and metamorphosed volcanic rocks using immobile elements. *Chemical Geology*, **21**, 291-306.

Green TH, Sie SH, Ryan CG, Cousens DR (1989) Protonmicroprobe-determined partitioning of Nb, Ta, Zr, Sr and Y between garnet, clinopyroxene and basaltic magma at high pressure and temperature. *Chemical Geology*, **74**, 201-216.

Grikurov GE, Krylov AY, Polyakov MM, Tsovbin YN (1970) Age of rocks in the northern part of Antarctic Peninsula and on the South Shetland Islands (K-Ar data). *Bulletin Soviet Antarctic Expeditions*, **80**, 30-39 (in Russian).

Gromet LP, Dymek RF, Haskin LA, Korotev RL (1984) The "North American Shale Composite": its compilation, major and trace element characteristics. *Geochimica et Cosmochimica Acta*, **48**, 2469-2482.

Hawkesworth C, Turner S, Peate D, McDermott F, van Calsteren P (1997) Elemental U and Th variations in island arc rocks: implications for U-series isotopes. *Chemical Geology*, **139**, 207-221.

Herron EM, Tucholke BE (1976) Seafloor magnetic patterns and basement structure in the southeastern Pacific. In: *Initial Reports of the Deep Sea Drilling Project, US Government Printing Office, 35, 263-278, Washington D.C.*

Herve F, Loske W, Miller H, Pankhurst RJ (1991) Chronology of provenance, deposition and metamorphism of deformed fore-arc sequence, southern Scotia arc. In: Thomson MRA, Crame JA, Thomson JW (Eds.)**.** *Geological Evolution of Antarctica***,** Cambridge University Press, 429-435.

Hobbs GJ (1968) The geology of the South Shetland Islands, IV. The geology of Livingston Island. *British Antarctic Survey, Scientific Reports,* **47**, 1-34.

Hofmann AW, Jochum KP, Seufert M, White WM (1986) Nb and Pb in oceanic basalts: New constraints on mantle evolution. *Earth and Planetary Science Letters*, **79**, 33-45.

Irvine TN, Baragar WRA (1971) A guide to the chemical classification of the common volcanic rocks. *Canadian Journal of Earth Science*, **8**, 523-548.

Kamenov BK (1997) Geochemistry and petrology of the Hesperides Point Intrusion, Hurd Peninsula, Livingston Island. In: Ricci C (ed.), *Geological Evolution and Processes*, *Terra Antarctica*. Siena, 341-352.

Kamenov BK (1999a) The dykes of Hurd Peninsula, Livingston Island - indicators of the geodynamic evolution in South Shetland Islands. *Abstracts of the 8-th International Symposium on Antarctic Earth Sciences*. Wellington, New Zealand, 5-10 July 1999, 188-189.

Kamenov BK (1999b) The dykes of Hurd Peninsula, Livingston Island - significant tracers of the tectono-magmatic history in South Shetland Magmatic Arc. Polish Polar Studies, *XXVI Polar Symposium*, Lublin, June, 1999, 111-112.

Kamenov BK (2004) The olivine basalts from Livingston Island, West Antarctica: Petrology and geochemical comparisons. *Geochemistry, Mineralogy and Petrology, Sofia,* **41**, 71-98.

Kamenov BK, Zheng X, Dimov D, Pimpirev C (2005) The isolated plutons in Hurd Peninsula, Livingston Island, Antarctica: Petrological and geochronological evidences of their affiliations to Barnard Point Batholith. *Geochemistry, Mineralogy and Petrology*, Sofia, **42**, 67-86.

Kraus S (2005) Magmatic dyke systems of the South Shetland Islands volcanic arc (West Antarctica): Reflections of the geodynamic history. PhD thesis published on line (http://edoc.ub.uni-muenchen.de/archive/00003827/). Als Dissertation eigenreicht au der Fakultät für Geowissenschaften Ludwig-Maximilians-Universität Munchen., Munich University Library, 160 p.

Kraus S, McWiliams M, Pecskay Z (2007) New ^{40}Ar/^{39}Ar and K/Ar ages of dikes in the South Shetland Islands (Antarctic Peninsula). *U.S. Geological Survey and the National Academies; USGS OF-2007-1047, Short Research Paper 035*; doi: 10.3133/0f2007-1047.srp035.

LeMaitre RW (Ed.) (2002) Igneous rocks: a classification and glossary of terms. Recommendations of the International Union of Geological Sciences subcommision on the systematics of igneous rocks. *Cambridge University Press*, 252 p.

Leterrier,Y, Maury RC, Thonon P, Girard D, Marshal M (1982) Clinopyroxene composition as a method of identification of the magmatic affinities of paleo-volcanic series. *Earth and Planetary Science Letters*, **59**, 139-154.

Mac Lean WH, Barrett TJ (1993) Lithogeochemical techniques using immobile elements. *Journal of Geochemical Exploration*, **48**, 109-133.

Mc Donough WF, Sun SS (1995) The composition of the Earth. *Chemical Geology*, **120**, 223-253.

Miller H, Loske W, Kramm U (1987) Zircon provenance and Gondwana reconstruction. U-Pb data of detrital zircons from Triassic Trinity Peninsula Formation metasandstowns. *Polarschung,* **57**, 59-69.

Miyashiro A (1974) Volcanic rock series in island arcs and active continental margins. *American Journal of Science*, **274**, 321-355.

Mysen BO, Kushiro I (1977) Compositional variations of coexisting phases with degree of melting of peridotite in the upper mantle. *American Mineralogist*, **62**, 843-856.

Nichols GT, WylliePJ, Stern CR (1994) Subduction zone melting of pelagic sediments constrained by melting experiments. *Nature*, **371**, 785-788.

Onuma N (1981) Sr/Ca – Ba/Ca systematics on eucrite parent body, the Moon and the Earth. *Proceedings of the 14th ISAS Lunar Planetary Symposium*, The Institute of Space and Austronautical Science, Tokyo, 334-340.

Ouyang S, Deng X, Shen Y, Zheng X, Liu X (2000) Late Triassic plant microfossils from Miers Bluff Formation of Livingston Island, South Shetland Islands. *Antarctic Science*, **12** (2), 217-228.

Pearce JA, Parkinson IJ (1993) Trace element models for mantle melting: application to volcanic arc petrogenesis. In: Prichard HM, Alabaster T, Harrison NBW, Neary CR (Eds.) *Magmatic Processes and Plate Tectonics*. Geol. Soc. London, Spec. Public., **76**, 373-403.

Peccerillo AS, Taylor SR (1976) Geochemistry of Eocene calc-alkaline volcanic rocks from the Kastamonu area, Northern Turkey. *Contributions to Mineralogy and Petrology*, **58**, 63-81.

Pimpirev C, Stoykova K, Ivanov M, Dimov D (2006) The sedimentary sequences of Hurd Peninsula, Livingston Island, South Shetland Islands: part of the Late Jurassic- Cretaceous depositional history of the Antarctic Peninsula. In: Fuetterer DK, Damaske D, Kleinschmidt G, Miller H, Tessensohn F (Eds.), *Antarctica Earth Sciences*, **9**, (ISBN: 3-540-30673-0), 249-253.

Plank T, Langmuir CH (1998) The chemical composition of subducting sediment and its consequences for the crust and mantle. *Chemical Geology*, **145**, 325-394.

Plank T, White W (1995) Nb and Ta in arc and mid-ocean ridge basalts. *EOS, Trans. AGU*, **76**, 655 p.

Pankhurst RJ (1983) Rb-Sr constraints on the age of basement rocks of the Antarctic Peninsula. In: Oliver, R.L., P.R. James, J.B. Jago (Eds.): Antarctic Earth Science – proceedings of the fourth international symposium on Antarctic Earth Sciences, Adelaide, South Australia. *Australian Academy of Science, Canberra /Cambridge Univ. Press*, 367-371.

Rex DC (1976) Geochronology in relation to the stratigraphy of the Antarctic Peninsula. *British Antarctic Survey Bulletin*, **43**, 49-58.

Rudnick RL, Gao S (2003) Composition of the continental crust. In: Rudnick RL (Ed.): *Treatise on geochemistry*, v. **3**, *The Crust,* Elsevier Ltd., I-64.

Schweitzer J, Kröner A (1985) Geochemistry and petrogenesis of Early Proterozoic intracratonic volcanic rocks of the Ventersdorp Supergroup, South Africa. *Chemical Geology*, **51**, 265-288.

Smellie JL (2001) Lithostratigraphy and volcanic evolution of Deception Island, South Shetland Islands. *Antarctic Science*, **13**, 188-209.

Smellie JL, Pankhurst RJ, Thomson MR, Davies RES (1984) The geology of the South Shetland Islands: VI. Stratigraphy, geochemistry and evolution. *British Antarctic Survey Bulletin*, **87**, 1-85.

Smellie JL, Liesa M, Munoz JA, Sabàt F, Pallàs R, Willan RCR (1995) Lithostratigraphy of volcanic and sedimentary sequences in central Livingston Island, South Shetland Islands. *Antarctic Science*, **7**, 1, 99-113.

Smellie JL, Pallàs R, Sabàt F, Zheng X (1996) Age and correlation of volcanism in central Livingston Island, South Shetland Islands: K-Ar and geochemical constraints. *Journal of South American Earth Sciences,* **9**, 265-272.

Stoykova K, Pimpirev C, Dimov D (2002) Calcareous nannofossils from the Miers Bluff Formation (Livingston Island, South Shetland Islands, Antarctica): First evidence for a Late Cretaceous age. *Journal of Nannoplankton Research*, **24**, 2, 211-214.

Sun SS, McDonough WF (1989) Chemical and isotopic systematics of oceanic basalts: Implications for mantle composition and processes. In: Saunders AD, Norry MJ (Eds), *Magmatism in the Ocean Basins*. Special Publications, Geological Society London, **42**, 313-345.

Tatsumi Y, Hamilton DL, Nesbitt RW (1986) Chemical characteristics of fluid phase released from a subducted lithosphere and origin of arc magmas: evidence from high-pressure experiments and natural rocks. *Journal of Volcanology Geothermal Research*, **29**, 293-309.

Tatsumi Y, Eggins S (1995) *Subduction Zone Magmatism.* Blackwell Science, Massachusetts, 211 p.

Tera F, Eugster O, Burnett DS, Wasenbury GI (1970) Comparative study of Li, K, Cs, Sr and B abundances in achondrites and Apollo 11 lunar samples. *Proceedings Apollo 11 Lunar Scientific Conference*, **2**, 1637-1657.

Turner SP, Hawkesworth CJ (1997) Constraints on flux rates and mantle dynamics beneath island arcs from Tonga-Kermadek lava geochemistry. *Nature*, **389**, 568-573.

Turner SP, Hawkesorth CJ, van Calsteren P, Heath E, Macdonald R, Black S (1996) U-series isotopes and destructive plate margin magma genesis in the Lesser Antilles. *Earth and Planetary Science Letters*, **142**, 191-207.

Turner SP, Hawkesorth CJ, Rogers NW, Barrett J, Worthington T, Hergt J, Pearce J, Smith I (1997) ^{238}U-^{230}Th disequilibria, magma petrogenesis, and flux rates beneath the depleted Tonga-Kermadec island arc. *Geochimica et Cosmochimica Acta*, **61**, 4855-4884.

Turner SP, George RMM, Evans PJ, Hawkesworth CJ, Zellmer GF (2000) Time-scales of magma formation, ascent and storage beneath subduction zone volcanoes. *Philosophical Transactions of the Royal Society of London*, A, **358**, 1443-1464.

Veit A (2002) Volcanology and geochemistry of Pliocene to Recent volcanics on both sides of the Bransfield Strait/West Antarctica. *Reports on Polar and Marin Research. Alfred Wagener Institute for Polar and Marine Research,* Bremerhaven, 420, 177.

Willan RCR (1994) Structural setting and timing of hydrothermal veins and breccias on Hurd Peninsula, South Shetland Islands: a possible volcanic-related epithermal system in deformed turbidites. *Geological Magazine*, **131**, 465-483.

Willan RCR, Kelley SP (1999) Mafic dike swarms in the South Shetland Islands volcanic arc: Unraveling multiepisodic magmatism related to Subduction and continental rifting. *Journal of Geophysical Research*, **104**, 23051-23068.

Willan RCR, Pankhurst RJ, Herve F (1994) A probable Early Triassic age for the Miers Bluf Formation, Livingston Island, South Shetland Islands. *Antarctic Science*, **6**, 401-408.

Wilson M (1989) *Igneous Petrogenesis: A Global Tectonic Approach.* Kluwer Acad. Pub., Dordrecht, 466 p.

Winchester JA, Floyd PA (1977) Geochemical discrimination of different magma series and their differentiation products using immobile elements. *Chemical Geology*, **20**, 325-343.

Woodhead J, Eggins S, Gamble J (1993) High field strength and transition element systematics in island arc and back-arc basin basalts: evidence for multiphase melt extraction and a depleted mantle wedge. *Earth and Planetary Science Letters*, **114**, 491-504.

Zheng X, Liu X (1997) Systematic covariation of Sr, Ba, Ca elements in Cenozoic volcanic rocks on the Fildes Peninsula, West Antarctica, and its relation to petrogenesis. *Antarctic Research*, **2**, 1, 30-38.

Zheng X, Kamenov BK, Sang H, Monchev P (2003) New radiometric dating of the dykes from the Hurd Peninsula, Livingston Island, South Shetland Islands. *Journal of South American Earth Sciences*, **15**, 925-934.

Accepted May 09, 2008
Приета на 09. 05. 2008 г.

Appendix

Foto 1. Bulgarian Antarctic base, constructed on the dykes of pulses IV (basalt) and V (basaltic andesite)

Foto 2. Dyke of basalt from pulse IV cutting Miers Bluff Formation